DEPARTMENT OF CIVIL ENGINEERING
COLLEGE OF ENGINEERING AND TECHNOLOGY
OLD DOMINION UNIVERSITY
NORFOLK, VIRGINIA 23529

TWO-DIMENSIONAL SEQUENTIAL AND CONCURRENT FINITE ELEMENT ANALYSIS OF UNSTIFFENED AND STIFFENED ALUMINUM AND COMPOSITE PANELS WITH HOLE

By

Zia Razzaq, Principal Investigator

Venkatesh Prasad, Graduate Student

Final Report
For the period ended March 31, 1988

Prepared for the
National Aeronautics and Space Administration
Langley Research Center
Hampton, Virginia 23665

Under
Research Grant NAG-1-438
Dr. Olaf O. Storaasli, Technical Monitor
SDD-Structural Mechanics Branch

July 1988

DEPARTMENT OF CIVIL ENGINEERING
COLLEGE OF ENGINEERING AND TECHNOLOGY
OLD DOMINION UNIVERSITY
NORFOLK, VIRGINIA 23529

TWO-DIMENSIONAL SEQUENTIAL AND CONCURRENT FINITE ELEMENT ANALYSIS OF UNSTIFFENED AND STIFFENED ALUMINUM AND COMPOSITE PANELS WITH HOLE

By

Zia Razzaq, Principal Investigator

Venkatesh Prasad, Graduate Student

Final Report
For the period ended March 31, 1988

Prepared for the
National Aeronautics and Space Administration
Langley Research Center
Hampton, Virginia 23665

Under
Research Grant NAG-1-438
Dr. Olaf O. Storaasli, Technical Monitor
SDD-Structural Mechanics Branch

Submitted by the
Old Dominion University Research Foundation
P. O. Box 6369
Norfolk, Virginia 23508-0369

July 1988

ACKNOWLEDGEMENT

The guidance and moral support provided by Dr. Olaf O. Storaasli has been of immense help. The participation of Jonathan B. Ransom in the project has also provided additional incentive for achieving convergence for some of the results. Sincere thanks are due to Dr. Jefferson W. Stroud and Dr. James H. Starnes, Jr. for providing motivation and criticism during the course of this work. The research was supported in part by NASA Grant NAG1-438.

TWO-DIMENSIONAL SEQUENTIAL AND CONCURRENT FINITE ELEMENT ANALYSIS OF UNSTIFFENED AND STIFFENED ALUMINUM AND COMPOSITE PANELS WITH HOLE

By

Zia Razzaq[1] and Venkatesh Prasad[2]

ABSTRACT

The results of a detailed investigation of the distribution of stresses in aluminum and composite panels subjected to uniform end shortening are presented. The focus problem is a rectangular panel with two longitudinal stiffeners, and an inner stiffener discontinuous at a central hole in the panel. The influence of the stiffeners on the stresses is evaluated through a two-dimensional global finite element analysis in the absence or presence of the hole. Contrary to the physical feel, it is found that the maximum stresses from the global analysis for both stiffened aluminum and composite panels are greater than the corresponding stresses for the unstiffened panels. The inner discontinuous stiffener causes a greater increase in stresses than the reduction provided by the two outer stiffeners. A detailed layer-by-layer study of stresses around the hole is also presented for both unstiffened and stiffened composite panels. A parallel equation solver is used for the global system of equations since the computational time is far less than that using a sequential scheme. A parallel Choleski method with up to 16 processors is used on Flex/32 Multicomputer at NASA Langley Research Center. The parallel computing results are summarized and include the computational times, speedups, bandwidths, and their inter-relationships for the panel problems. It is found that the computational time for Choleski method decreases with a decrease in bandwidth, and better speedups result as the bandwidth increases.

[1]Professor, Department of Civil Engineering, Old Dominion University, Norfolk, Virginia 23529. Fellow, ASCE.

[2]Graduate Student, Department of Civil Engineering, Old Dominion University, Norfolk, Virginia 23529.

TABLE OF CONTENTS

I. INTRODUCTION

There is an ever increasing need for accurate and high speed numerical computations to evaluate the stress distributions in aerospace structures. Furthermore, the constant demand to reduce the weight/stiffness ratios for such structures has made the use of composite materials an attractive option in comparison to aluminum alloys. The process of routine stress analysis as well as that of reducing the structural weight is considerably improved through a detailed global and/or local stress analysis of structural components in the presence or absence of discontinuities. This report presents the outcome of a two-dimensional sequential and concurrent finite element stress analysis of unstiffened and stiffened rectangular panels with and without a central hole. Both aluminum and composite panels are investigated. Such panels have wide applications in wing and fuselage structures of aircraft. Holes are drilled into panels used in aerospace vehicles to facilitate bolting and riveting to primary structure, or to provide access to the interior of wings.

The buckling and failure mechanisms for rectangular panels with and without stiffeners and a central hole are studied by some researchers. Examples include the experiments by Starnes and Williams (reference 1), and Knauss and Henneke (reference 2) on composite panels. A limited number of three-dimensional finite element analyses of unstiffened rectangular panels with hole are available. References 3 through 7 are representative examples published in over a decade, and contain results for composite panels subjected to uniform compressive or tensile boundary stresses. Hirai, Wang, and Pilkey (reference 8) presented a finite element zooming technique employing static condensation and structural reanalysis. They have reported stress concentration factors with various types of local meshes for a rectangular steel panel with hole and subjected to a uniaxial tensile boundary stress. A review of the existing literature indicates that no detailed pre-buckling numerical

stress distributions are published in the past for rectangular panels with stiffeners and a central hole.

The objective of this report is to study and compare the distribution of stresses and maximum stresses near the hole in unstiffened and stiffened, aluminum and composite panels, without and with a hole, when subjected to uniform end shortening. The maximum stress values based on global analysis for both stiffened aluminum and composite panels are found to be greater than the corresponding values for unstiffened ones. This phenomenon is contrary to the common belief that the stiffeners reduce such stresses. Hence, a further investigation became necessary, and was accomplished through the identification of the individual effects of the inner and outer stiffeners on the maximum stresses. Also, only a limited amount of work has been carried out in the past on finite element stress analysis problems through the use of computationally efficient parallel solvers for simultaneous equations. The performance of a parallel equation solver based on Choleski method (references 9 and 10) is also evaluated for the panel problems considered herein.

II. DESCRIPTION OF PROBLEMS

Figure 1 shows six types of panels analyzed in this paper. Figures 1(a) and 1(b) show rectangular panels without, and with stiffeners, respectively, in the absence of a hole. The panels shown in Figures 1(c) through 1(f) have a central hole. The panel in Figure 1(c) is unstiffened, while those in Figures 1(d) through 1(f) are provided with one, two, and three stiffeners, respectively, as shown. The problems shown were solved using the NASA Langley Computational Structural Mechanics testbed software system (reference 11).

The finite element discretizations for the panel skin and stiffeners are shown in Figure 2. The overall panel dimensions L_1 and L_2; the distance between panel edge and outer stiffener, B_e, and the distance between the inner and outer stiffeners, B_s, are shown in Figure 2(a). Each stiffener has a height of H_s as indicated in Figure 2(b). In these figures, the global axes are indicated as X_1, X_2, and X_3. The discretization in the region around the hole used in the global analysis is shown in Figure 2(c). The global model in the region around the hole, and the local model around the hole are shown in Figure 2(d). The discretization for the stiffened panel with a hole is shown in Figure 2(e). Quadrilateral elements are used for the panels considered, except for the panels without a hole in which case additional triangular elements are used to fill in the region of the hole. Each node has two translational degrees-of-freedom along the X_1 and X_2 axes, for the unstiffened panels. However, for the stiffened panels, each node has six degrees-of-freedom, namely, three translations and three rotations relative to the X_1, X_2, and X_3 axes.

The following dimensions are adopted for the panel skin and stiffeners: L_1 = 30.0 in.; L_2 = 11.5 in.; R = 1.0 in.; B_s = 4.5 in.; B_e = 1.25 in.; H_s = 1.4 in., and A = 4.0 in. The thickness of the aluminum panel is taken as 0.1 in. for both the panel skin and each stiffener. The thickness of the composite panel skin is 0.1375 in. for a total of 25 plies, and that of each

composite stiffener is 0.132 in. for a total of 24 plies. The Young's modulus, and Poisson's ratio for aluminum are taken as 10,000 ksi, and 0.30, respectively. The material of the composite panels is graphite-epoxy (T300/5208) with the following mechanical properties: E_1 = 19,000 ksi; E_2 = 1,890 ksi; μ_{12} = 0.38, and G_{12} = 930 ksi, as adopted in reference 2.

Each panel is subjected to a uniform edge shortening of 0.1 in. in the longitudinal (X_1) direction, imposed at the face OS as shown in Figure 2(a). The boundary conditions adopted for the unstiffened, and stiffened panels are summarized in Tables 1, and 2, respectively.

III. STRESS DISTRIBUTIONS

In this section, the results are given for the various types of panels shown in Figure 1. Dimensionless contour plots for the principal compressive stresses are presented for a quarter of these panels, based on the global analysis. Contours are also drawn for the region around the hole for the unstiffened panel, based on the local analysis. For the stiffened panel, the maximum midsurface shear stress distribution at the location of the stiffeners is also given. Both aluminum and composite panels are considered. Furthermore, the influence of inner and outer stiffeners on the stresses is identified.

3.1 Stress Distributions in Aluminum Panels

3.1.1 Unstiffened and Stiffened Aluminum Panels without Hole

The total degrees-of-freedom (DOF) for unstiffened, and stiffened panels without hole are 554, and 2346, respectively. Table 3 presents the dimensionless principal stresses, $\bar{\sigma}_2$, given by the ratio of the principal compressive stress, σ_2, and the far field (boundary) stress, σ_0, for the panels shown in Figures 1(a) and 1(b). The values are summarized in the table for various locations identified by the coordinates X_1, X_2 indicated in Figure 2. The corresponding stresses in the stiffeners are summarized in Table 4.

3.1.2 Unstiffened and Stiffened Aluminum Panels with Hole

The $\bar{\sigma}_2$ contours for the unstiffened panel with hole based on a 552 DOF global model are presented in Figure 3(a). The contours based on the local analysis for the region around the hole are shown in Figure 3(b). The local analysis procedure is based on imposing an interpolated displacement field for the region around the hole . The stress concentration factors (SCF) for the global and local analysis are 2.74, and 3.00, respectively. Figure 4(a) shows the stress contours for the stiffened panel skin analyzed globally in which the outer

and inner stiffener locations are also indicated. Figures 4(b) and 4(c) show the contours for these stiffeners. The resulting SCF for the stiffened aluminum panel is 2.89.

It is interesting to note that the SCF for the stiffened panel is greater than that of the unstiffened one. The reason for this phenomenon is explained later in this report. The outer stiffeners develop higher stresses than those in the inner one. Also, a substantial part of the inner stiffener is stress-free. The midsurface maximum shear stress (τ_{max}) distribution for the panel at the location of both inner and outer stiffeners is shown in Figure 5 as a function of the distance X_h from the center of the hole. The τ_{max} exhibits a greater variation along the panel length at the inner stiffener location in comparison to that observed for the outer stiffener location. The reason may be attributable to a more dramatic variation in normal stresses for the inner stiffener in the panel longitudinal direction as compared to that for the outer stiffeners, as may be seen readily from the nature of the contours in Figures 4(b) and 4(c).

3.2 Stress Distributions in Composite Panels

The results for various types of composite panels shown in Figure 1 are presented in this section. Dimensionless contours for the principal compressive stress resultants based on global analysis are presented for a quarter of each panel shown in Figures 1(c) and 1(f). Contours are also drawn for the region around the hole for the unstiffened panel based on the local analysis. Tables showing the variation of principal stresses and maximum shear stresses around the hole and through the 25 layers are presented for both stiffened and unstiffened panels. Also included are the plots showing the variation of principal stresses and maximum shear stresses around the hole in the layer with highest value of stresses. In addition, plots are presented for the variation of these stresses through the layers and at the node with maximum stresses.

3.2.1 Unstiffened and Stiffened Panels without Hole

Table 5 presents the dimensionless principal stress resultant, $\bar{\sigma}_{sr2}$, given by the ratio of the principal compressive stress resultant, σ_{sr2}, and the far field (boundary) stress resultant, σ_{sro}, for the panels shown in Figures 1(a) and 1(b). The stress resultant, σ_{sr}, is defined by:

$$\sigma_{sr} = \Delta t \, \Sigma f_i$$

in which Δt is the thickness of one ply, f_i is the stress in the i-th ply, and the summation is over N plies. The dimensionless stress resultants are summarized in the table for various locations identified by the coordinates X_1 and X_2 indicated in Figure 2. The corresponding stress resultants in the stiffeners are summarized in Table 6. It is seen that in the unstiffened panel $\bar{\sigma}_{sr2}$ ranges from 1.00 to 1.13, while in the stiffened panel, it ranges from 0.96 to 1.05. The corresponding values for the stiffener are in the range from 1.09 to 1.39.

3.2.2 Unstiffened Panel with Hole

Figure 6(a) shows the dimensionless stress resultant $\bar{\sigma}_{sr2}$ contours for the 552 DOF global model. The contours based on the local analysis for the region around the hole are shown in Figure 6(b). The maximum $\bar{\sigma}_{sr2}$ value for the global and local analysis are 1.74 and 1.90, respectively. Table 7 presents the variation of maximum principal stress, σ_1, around the hole for all the 25 layers of the panel skin. It is seen that the σ_1 value is maximum at D" for a -45° ply-orientation. Figures 9 and 10 show the variation of σ_1 around the hole, and through the layers at D", respectively. The maximum value of σ_1 exists at D", while the minimum values are at C' and C". It is also seen that the same values of σ_1 exist for a given orientation through the layers at each node. Table 8 presents the variation of minimum principal stress, σ_2, around the hole for all the 25 layers of the panel skin. The maximum value is seen at C for 0° ply-orientation. Figure 11 and 12 show the variation of

σ_2 around the hole, and through the layers at C′, respectively. It is seen that the maximum values of σ_2 are at C and C″, and the same values of σ_2 exist for a given orientation through the layers at each node. Table 9 shows the variation of maximum shear stress, τ_{max}, around the hole for all the 25 layers of the panel skin. Here too, the maximum value is at C′ for 0° ply-orientation. Figures 13 and 14 show the variation of τ_{max} around the hole, and through the layers, respectively. The maximum values are at C and C″ and the same values of τ_{max} exist for a particular ply-orientation through the layers at each node.

3.2.3 Stiffened Panel with Hole

The dimensionless stress resultant $\bar{\sigma}_{sr2}$ contours for the panel skin of the 2328 DOF global model are presented in Figure 7(a). The stress resultant contours for the stiffeners are shown in Figures 7(b) and 7(c). The maximum $\bar{\sigma}_{sr2}$ for the global analysis is found to be 1.8. The distribution of the maximum shear stress resultants τ_{max}, for the inner and outer stiffeners is shown in Figure 8. A rapid variation is found at the inner stiffener location except for the region close to the panel edge, that is, as X_h approaches 15 in. Its variation at the outer stiffener location is relatively small. Table 10 shows the variation of maximum principal stress, σ_1, around the hole for all the 25 layers of the panel skin. The maximum value of σ_1 is seen at D″ on the bottom-most layer (25th) with a ply-orientation of 45°. Figure 15 shows the variation of σ_1 around the hole for the 25th layer, and Figure 16, the variation through all the layers at D″. The highest value of σ_1 is at D″, while the lowest value is at C″. Table 11 presents the variation of minimum principal stress, σ_2, around the hole for all the 25 layers of the panel skin. The maximum value of σ_2 is seen at C′ on the third layer, with a ply-orientation of 0°. Figure 17 shows the σ_2 variation around the hole for the 3rd layer, and Figure 18, the variation through all the layers at C′. The maximum value of σ_2 is at C′, while the minimum is at D″. Table 12 shows the variation of maximum shear stress, τ_{max}, around the hole for all the 25 layers of the panel skin. The

maximum value of τ_{max} is found at D" on the 25th layer with a 45° ply-orientation. Figure 19 shows the τ_{max} variation around the hole for the 25th layer, and Figure 20 the variation through all the layers at D". The maximum value of τ_{max} is at D", while the minimum is at a location half-way between C" and D".

3.2.4 Nature of Stresses in Composite Panels

The unstiffened panel without a hole exhibits a fairly uniform stress resultant throughout, except at the center of the panel where it is nearly 13% more than the surrounding stress resultants. In the stiffened composite panel, a nearly uniform stress resultant distribution in the range from 0.95 to 1.05 of the boundary stress resultant is seen. The stiffeners exhibit larger values of upto 1.39. In the unstiffened panel high stress gradients exist in the vicinity of the hole and are more prominent along C'C as seen in the Figure 7. The stiffened panel with a hole has higher stress resultants at C' than that in the unstiffened one. The outer stiffeners develop higher stress resultants than the inner stiffeners. Furthermore, as observed in the case of aluminum stiffener, the composite stiffener also possesses a region with little or no stress resultant. The τ_{max} variation is more in the inner stiffener location than at the outer stiffener location due to considerable variation of normal stress resultants in the panel longitudinal direction.

The maximum values of principal stresses σ_1 and σ_2 occur on different layers for both unstiffened and stiffened composite panels with a hole. The unstiffened panel has the highest values of σ_2 and maximum shear stress, τ_{max}, on the same layer, while the stiffened panel has the maximum values of σ_1 and τ_{max} on the same layer. The stresses are the same for a particular ply-orientation for the unstiffened panel whereas they are different for each layer for the stiffened one.

For both the unstiffened and stiffened panels, the σ_1 value is maximum at the location D", but it exists on the -45° ply-orientation for the former and 45° for the latter. The σ_2

distribution around the hole for the unstiffened panel shows a symmetry about $D''D'$. The maximum value of σ_2 is at C' and C'' while its minimum value is at D'' for both the cases. For the stiffened panel, the σ_2 distribution through the layers has its maximum values on the third layer, with a 0° ply-orientation. The same is true for the unstiffened panel except that it is repeated for each ply with 0° orientation. The τ_{max} distribution around the hole is symmetrical about $D''D'$ for only the unstiffened panel with its maximum value at C' and C'' on the third layer, and repeated for each layer with the same orientation. The stiffened panel develops the maximum value in the 25th layer at D''.

3.3 Influence of Inner and Outer Stiffeners on Stresses

As mentioned previously in this report, the SCF and $(\bar{\sigma}_{sr2})_{max}$ values for stiffened aluminum and composite panels, respectively, were found to be greater than the corresponding values for the unstiffened ones. To understand the cause of this phenomenon global analyses of the panels shown in Figures 1(d), and 1(f) were conducted while utilizing 1,920 DOF and 2,070 DOF model, respectively. The resulting SCF and $(\bar{\sigma}_{sr2})_{max}$ values for aluminum and composite panels, respectively, together with those obtained previously for the panels shown in Figures 1(a) and 1(f), are summarized in Tables 13 and 14.

The results in Table 13 reveal that when an aluminum panel is "stiffened" by the inner stiffener only (Case 2), the SCF is 2.93, that is about 7% greater than that of the unstiffened panel (Case 1). The inner stiffener appears to be acting as a nearly direct load-transfer unit between the loaded boundaries and the hole thereby causing a further increase in the maximum compressive stresses. The SCF value for the aluminum with all three stiffeners (Case 4) is found to be 2.89 which is also greater than that for the unstiffened one. However, a comparison of the SCF values for Cases 1,2 and 4 leads to the conclusion that the outer two stiffeners must be introducing a beneficial effect on the maximum stresses. This conclusion was confirmed through the analysis of the panel with only the

outer stiffeners (Case 3) which provided an SCF of 2.69, that is, lower than that for the unstiffened panel.

The results in the Table 14 reveal that for the panel with only the middle stiffener (case 2), the maximum dimensionless stress resultant, $(\bar{\sigma}_{sr2})_{max}$, is 1.84 or 6% greater than that for the unstiffened panel. This increase is attributed to the middle stiffener acting as a direct load-transfer unit between the loaded boundaries and the hole causing a further increase in the maximum compressive stress resultants. The beneficial effect of introducing two outer stiffeners (Case 3) is evident from $(\bar{\sigma}_{sr2})_{max}$ value of 1.66, which is 5% less than that for the unstiffened one. The adverse effect of the middle stiffener is also seen for the panel with all the three stiffeners (Case 4). Here, the $(\bar{\sigma}_{sr2})_{max}$ value is 1.80, which is 4% greater than that for the unstiffened one.

IV. Concurrent Processing

All of the global analysis computations for the aluminum and composite panels investigated in this study were carried out on a parallel computer (Flex/32 Multicomputer, reference 2.) installed at NASA Langley Research Center. For each problem, the global system of equations for finding the nodal displacements was solved on up to 16 parallel processors using the Choleski method (reference 1). Table 15 gives the computational times and speedups for the unstiffened and stiffened aluminum panels with hole. Table 16 gives similar results for the aluminum panel with hole and inner or outer stiffeners. The computational time and speedup results for the unstiffened and stiffened panels without hole was found to be quite similar to that given in Table 15 for the panels with hole. Similarly, the results for the composite panels were found to be practically the same as that for the aluminum panels. As illustrations, Figures 21 and 22 present the relationships between the computational time (T_c) versus the number of parallel processors corresponding to the results given in Table 15. The associated speedup curves are plotted in Figure 23 and compared to the ideal relationship. The advantage of concurrent processing for solving finite element analysis problems of the type considered herein is quite obvious from these figures.

The bandwidths for the global stiffness matrix for the panels shown in Figures 1(c) through 1(f) are found to be 70, 195, 218, and 240, respectively. Figure 24 shows the variation of the computational time T_c, given in Tables 15 and 16, with matrix bandwidth B_m, and the number of processors N. The curves in this figure indicate that the steepness of the T_c-B_m relationship decreases with an increase in N. This may be attributed to increased inter-processor communication time losses.

V. CONCLUSIONS

The study of the distribution of stresses for unstiffened and stiffened, aluminum and composite panels has led to the following useful and interesting conclusions:

1. The maximum compressive stresses for composite panels are substantially smaller than those for aluminum panels.
2. Local analysis of panels provides a detailed and accurate distribution of stresses concentrated around the hole.
3. The outer stiffeners in the aluminum panel develop higher compressive stresses than does the inner one. This difference is even greater in the composite panel.
4. In both aluminum and composite panels, the maximum shear stress exhibits a greater variation along the panel length at the inner stiffener location in comparison to that observed for the outer stiffener location.
5. The maximum compressive stresses from the global analysis for both stiffened aluminum and composite panels are greater than the corresponding stresses for the unstiffened ones. The panels with only the inner stiffener develop greater stresses than those for the unstiffened panels. However, the outer two stiffeners cause a reduction in the stress values, although this reduction does not completely off-set the detrimental influence of the inner stiffener.
6. The layer-by-layer stress analysis shows that the maximum value of the principal compressive stress exists on the 0° ply-orientation for both stiffened and unstiffened composite panels. The maximum principal tensile stress exists on the -45° ply-orientation for the unstiffened panel, and on the bottom-most 45° ply-orientation for the stiffened panel. The largest value of the maximum shear stress occurs on the 0° ply-orientation for the unstiffened composite panel, and on the bottom most 45° ply-orientaion for the stiffened composite panel.
7. The computational time required by the Choleski method decreases as the number of processors is increased and decreases with the bandwidth.

VI. REFERENCES

1. Starnes, J.H., Jr., Williams, J.G., "Failure Characteristics of Graphite-Epoxy Structural Components Loaded in Compression," Mechanics of Composite Materials: Recent Advances, Proceedings of the Symposium, Blacksburg, VA, August 16-19, 1982, New York, Pergamon Press, 1983, pp. 283-306.

2. Knauss, J.F., Henneke, E.G., II, "The Compressive Failure of Graphite/Epoxy Plates with Circular Holes," Composites Technology Review, Vol. 3, VPI & SU, Blacksburg, Summer 1981, pp. 64-75.

3. Barker, R.M., Pryor, C.W., and Dana, J.R., "Stress Concentration near Holes in Laminates," Journal of the Engineering Mechanics Division, ASCE, Vol. 100, June, 1974, pp. 477-488.

4. Raju, I.S., and Crews, J.H., Jr., "Three-Dimensional Analysis of /0/90/s and /90/0/s Laminates with a Central Circular Hole, "Composites Technology Review, Vol. 4, Winter 1982, pp. 116-124.

5. Rybicki, E.F., and Schmueser, D.W., "The Comparison of LPT and Three-Dimensional Stress Distributions for a Laminated Plate Containing a Hole -- Laminar Plate Theory," Proceedings of the Second International Conference on Composite Materials, Toronto, Canada, April 16-20, 1978, Metallurgical Society of AIME, 1978, pp. 376-384.

6. Lucking, W.M., Hoa, S.V., and Sankar, T.S., "The Effect ofg Geometry on Interlaminar Stresses of $[0/90]_S$ Composite Laminates with Circular Holes," Journal of Composite Materials, Vol. 18, March 1984, pp. 188-198.

7. Lee, J.D., "Three Dimensional Finite Element Analysis of Layered Fiber-Reinforced Composite Materials," Computers and Structures, Vol.12, September 1980, pp. 319-339.

8. Hirai, I., Wang, P., and Pilkey, W.D., "An Exact Zooming Method for Finite Element Analyses," Research in Structural and Solid Mechanics-1982, NASA Conference Publication 2245, October 4-7, 1982.

9. Poole, E.L., Storaasli, O., Ortega, J.M., Cleary, A.J., and Vaughan, C.T., "Solution of Structural Analysis Problems on a Parallel Computer," Proceedings of the 29th AIAA/ASME/ASCE/AHS/ASC Structures, Structural Dynamics and Materials Conference, Williamsburg, Virginia, April 18-20, 1988.

10. Storaasli, O., Bostic, S., Patrick, M., Mahajan, U., Ma, S., "Three Parallel Computation Methods for Structural Vibration Analysis," Proceedings of the 29th AIAA/ASME/ASCE/AHS/ASC Structures, Structural Dynamics and Materials Conference, Williamsburg, Virginia, April 18-20, 1988.

11. Lotts,T. et al.,"Introduction to the CSM Testbed": NICE/SPAR, NASA TM-89096, 1986.

Table 1. Boundary Conditions for Unstiffened Panels
(u=unconstrained; c=constrained)

Deflection	Edges				Corners			
	OP	PQ	QS	SO	O	P	Q	S
ΔX_1	u	c	u	u	u	c	c	u
ΔX_2	u	u	u	u	u	u	c	c

Table 2. Boundary Conditions for Stiffened Panels
(u=unconstrained; c=constrained)

Deflection	Panel Skin								Stiffeners	
	Edges				Corners				Edges	
	OP	PQ	QS	SO	O	P	Q	S	KO	IJ
ΔX_1	u	c	u	u	u	c	c	u	u	c
ΔX_2	u	u	u	u	u	u	c	c	c	c
ΔX_3	u	c	u	c	c	c	c	c	c	c
θX_1	u	c	u	c	c	c	c	c	c	c
θX_2	u	c	u	c	c	c	c	c	c	c
θX_3	u	c	u	c	c	c	c	c	c	c

Table 3. Dimensionless Principal Stresses, $\bar{\sigma}_2$, for Aluminum Panels without Hole.

Location (inches)		Dimensionless Principal Stress, $\bar{\sigma}_2$	
X_1	X_2	Unstiffened (33333.2)*	Stiffened (33918.8)
0.00	0.00	1.00	1.00
0.00	5.75	1.00	0.99
0.00	11.50	1.00	1.02
15.00	0.00	1.00	0.98
15.00	5.75	1.00	0.98
15.00	11.50	1.00	0.98

* σ_0, psi

Table 4. Dimensionless Principal Stresses, $\bar{\sigma}_2$, for Stiffeners in Aluminum Panels without Hole

Location (inches)			Dimensionless Principal Stress, $\bar{\sigma}_2$
X_1	X_2	X_3	(33918.80)*
0.00	1.25	0.00	0.99
0.00	1.25	1.40	0.99
15.00	1.25	0.00	0.99
15.00	1.25	1.40	0.99
0.00	5.75	0.00	0.99
0.00	5.75	1.40	0.99
15.00	5.75	0.00	0.98
15.00	5.75	1.40	0.99
0.00	10.50	0.00	0.99
0.00	10.50	1.40	0.98
15.00	10.50	0.00	0.98
15.00	10.50	1.40	0.99

* σ_0, psi

Table 5. Dimensionless Principal Stress Resultants, $\bar{\sigma}_{sr2}$, for Composite Panels without Hole.

Location (inches)		Dimensionless Principal Stress Resultant, $\bar{\sigma}_{sr2}$	
		Unstiffened	Stiffened
X_1	X_2	(5135.87)*	(5344.77)
0.00	0.00	1.00	1.00
0.00	5.75	1.00	0.96
0.00	11.50	1.00	1.05
15.00	0.00	1.04	1.00
15.00	5.75	1.13	1.05
15.00	11.50	1.04	1.01

* σ_{sro}, ppi

Table 6. Dimensionless Principal Stress Resultants, $\bar{\sigma}_{sr2}$, for Stiffeners in Composite Panels without Hole

Location (inches)			Dimensionless Principal Stress Resultant
X_1	X_2	X_3	(5344.77)*
0.00	1.25	0.00	1.10
0.00	1.25	1.40	1.39
15.00	1.25	0.00	1.10
15.00	1.25	1.40	1.33
0.00	5.75	0.00	1.10
0.00	5.75	1.40	1.38
15.00	5.75	0.00	1.12
15.00	5.75	1.40	1.20
0.00	10.50	0.00	1.09
0.00	10.50	1.40	1.33
15.00	10.50	0.00	1.17
15.00	10.50	1.40	1.37

* σ_{sro}, ppi

Table 7. Maximum principal stresses around hole for various layers of unstiffened composite panel (psi)

J / θ°	1	2	3	4	5	6	7	8	9	10	11	12	13	14	15	16	J / θ°
45	50552.37	32970.15	17456.16	11925.35	-1621.11	-1323.72	333.71	19960.84	58137.94	34027.39	20594.74	10217.73	-1613.16	-392.66	1423.59	38265.45	45
-45	50553.37	38267.97	1423.72	-392.66	-1613.02	10219.38	20594.35	34026.01	58139.24	19963.06	338.88	-1323.75	-1621.19	11926.19	17457.15	32969.35	-45
0	11115.97	8028.16	1816.08	196.70	914.88	-1116.95	-269.23	6407.55	12488.00	6407.87	-268.88	-1116.77	914.76	196.63	1815.86	8027.86	0
0	11115.97	8028.16	1816.08	196.70	914.88	-1116.95	-269.23	6407.55	12488.00	6407.87	-268.88	-1116.77	914.76	196.63	1815.86	8027.86	0
-45	50553.37	38267.97	1423.72	-392.66	-1613.02	10219.38	20594.35	34026.01	58139.24	19963.06	338.88	-1323.75	-1621.19	11926.19	17457.15	32969.35	-45
45	50552.37	32970.15	17456.16	11925.35	-1621.11	-1323.72	333.71	19960.84	58137.94	34027.39	20594.74	10217.73	-1613.16	-392.66	1423.59	38265.45	45
0	11115.97	8028.16	1816.08	196.70	914.88	-1116.95	-269.23	6407.55	12488.00	6407.87	-268.88	-1116.77	914.76	196.63	1815.86	8027.86	0
0	11115.97	8028.16	1816.08	196.70	914.88	-1116.95	-269.23	6407.55	12488.00	6407.87	-268.88	-1116.77	914.76	196.63	1815.86	8027.86	0
0	11115.97	8028.16	1816.08	196.70	914.88	-1116.95	-269.23	6407.55	12488.00	6407.87	-268.88	-1116.77	914.76	196.63	1815.86	8027.86	0
45	50552.37	32970.15	17456.16	11925.35	-1621.11	-1323.72	333.71	19960.84	58137.94	34027.39	20594.74	10217.73	-1613.16	-392.66	1423.59	38265.45	45
-45	50553.37	38267.97	1423.72	-392.66	-1613.02	10219.38	20594.35	34026.01	58139.24	19963.06	338.88	-1323.75	-1621.19	11926.19	17457.15	32969.35	-45
0	11115.97	8028.16	1816.08	196.70	914.88	-1116.95	-269.23	6407.55	12488.00	6407.87	-268.88	-1116.77	914.76	196.63	1815.86	8027.86	0
0	11115.97	8028.16	1816.08	196.70	914.88	-1116.95	-269.23	6407.55	12488.00	6407.87	-268.88	-1116.77	914.76	196.63	1815.86	8027.86	0
0	11115.97	8028.16	1816.08	196.70	914.88	-1116.95	-269.23	6407.55	12488.00	6407.87	-268.88	-1116.77	914.76	196.63	1815.86	8027.86	0
-45	50553.37	38267.97	1423.72	-392.66	-1613.02	10219.38	20594.35	34026.01	58139.24	19963.06	338.88	-1323.75	-1621.19	11926.19	17457.15	32969.35	-45
45	50552.37	32970.15	17456.16	11925.35	-1621.11	-1323.72	333.71	19960.84	58137.94	34027.39	20594.74	10217.73	-1613.16	-392.66	1423.59	38265.45	45
0	11115.97	8028.16	1816.08	196.70	914.88	-1116.95	-269.23	6407.55	12488.00	6407.87	-268.88	-1116.77	914.76	196.63	1815.86	8027.86	0
0	11115.97	8028.16	1816.08	196.70	914.88	-1116.95	-269.23	6407.55	12488.00	6407.87	-268.88	-1116.77	914.76	196.63	1815.86	8027.86	0
0	11115.97	8028.16	1816.08	196.70	914.88	-1116.95	-269.23	6407.55	12488.00	6407.87	-268.88	-1116.77	914.76	196.63	1815.86	8027.86	0
45	50552.37	32970.15	17456.16	11925.35	-1621.11	-1323.72	333.71	19960.84	58137.94	34027.39	20594.74	10217.73	-1613.16	-392.66	1423.59	38265.45	45
-45	50553.37	38267.97	1423.72	-392.66	-1613.02	10219.38	20594.35	34026.01	58139.24	19963.06	338.88	-1323.75	-1621.19	11926.19	17457.15	32969.35	-45
0	11115.97	8028.16	1816.08	196.70	914.88	-1116.95	-269.23	6407.55	12488.00	6407.87	-268.88	-1116.77	914.76	196.63	1815.86	8027.86	0
0	11115.97	8028.16	1816.08	196.70	914.88	-1116.95	-269.23	6407.55	12488.00	6407.87	-268.88	-1116.77	914.76	196.63	1815.86	8027.86	0
-45	50553.37	38267.97	1423.72	-392.66	-1613.02	10219.38	20594.35	34026.01	58139.24	19963.06	338.88	-1323.75	-1621.19	11926.19	17457.15	32969.35	-45
45	50552.37	32970.15	17456.16	11925.35	-1621.11	-1323.72	333.71	19960.84	58137.94	34027.39	20594.74	10217.73	-1613.16	-392.66	1423.59	38265.45	45
J / θ°	1	2	3	4	5	6	7	8	9	10	11	12	13	14	15	16	J / θ°

Table 8. Minimum principal stresses around hole for various layers of unstiffened composite panel (psi)

θ \ J	1	2	3	4	5	6	7	8	9	10	11	12	13	14	15	16	J \ θ
45	5364.10	3736.57	- 1761.31	- 6094.23	-29115.46	-73510.96	-52004.36	2582.18	6345.70	2280.81	- 4613.85	- 8091.88	-28478.57	-53938.37	-19656.38	3556.98	45
-45	5364.05	3557.17	-19652.84	-53936.12	-28476.72	- 8092.01	- 4614.09	2280.54	6345.65	2582.49	-52001.54	-73506.98	-29113.79	- 6094.35	- 1761.57	3736.30	-45
0	-22127.42	-18966.05	-30253.34	-66397.49	-96564.11	-77686.97	-39101.51	-20050.32	-20352.12	-20049.75	-39102.79	-77686.88	-96562.81	-66398.24	-30253.42	-18966.63	0
0	-22127.42	-18966.05	-30253.34	-66397.49	-96564.11	-77686.97	-39101.51	-20050.32	-20352.12	-20049.75	-39102.79	-77686.88	-96562.81	-66398.24	-30253.42	-18966.63	0
-45	5364.10	3557.17	-19652.84	-53936.12	-28476.72	- 8092.01	- 4614.09	2280.54	6345.65	2582.49	-52001.54	-73506.98	-29113.79	- 6094.35	- 1761.57	3736.30	-45
45	5364.10	3736.57	- 1761.31	- 6094.23	-29115.46	-73510.96	-52004.36	2582.18	6345.70	2280.81	- 4613.85	- 8091.88	-28478.57	-53938.37	-19656.38	3556.98	45
0	-22127.42	-18966.05	-30253.34	-66397.49	-96564.11	-77686.97	-39101.51	-20050.32	-20352.12	-20049.75	-39102.79	-77686.88	-96562.81	-66398.24	-30253.42	-18966.63	0
0	-22127.42	-18966.05	-30253.34	-66397.49	-96564.11	-77686.97	-39101.51	-20050.32	-20352.12	-20049.75	-39102.79	-77686.88	-96562.81	-66398.24	-30253.42	-18966.63	0
0	-22127.42	-18966.05	-30253.34	-66397.49	-96564.11	-77686.97	-39101.51	-20050.32	-20352.12	-20049.75	-39102.79	-77686.88	-96562.81	-66398.24	-30253.42	-18966.63	0
45	5364.10	3736.57	- 1761.31	- 6094.23	-29115.46	-73510.96	-52004.36	2582.18	6345.70	2280.81	- 4613.85	- 8091.88	-28478.57	-53938.37	-19656.38	3556.98	45
-45	5364.10	3557.17	-19652.84	-53936.12	-28476.72	- 8092.01	- 4614.09	2280.54	6345.65	2582.49	-52001.54	-73506.98	-29113.79	- 6094.35	- 1761.57	3736.30	-45
0	-22127.42	-18966.05	-30253.34	-66397.49	-96564.11	-77686.97	-39101.51	-20050.32	-20352.12	-20049.75	-39102.79	-77686.88	-96562.81	-66398.24	-30253.42	-18966.63	0
0	-22127.42	-18966.05	-30253.34	-66397.49	-96564.11	-77686.97	-39101.51	-20050.32	-20352.12	-20049.75	-39102.79	-77686.88	-96562.81	-66398.24	-30253.42	-18966.63	0
0	-22127.42	-18966.05	-30253.34	-66397.49	-96564.11	-77686.97	-39101.51	-20050.32	-20352.12	-20049.75	-39102.79	-77686.88	-96562.81	-66398.24	-30253.42	-18966.63	0
-45	5364.10	3557.17	-19652.84	-53936.12	-28476.72	- 8092.01	- 4614.09	2280.54	6345.65	2582.49	-52001.54	-73506.98	-29113.79	- 6094.35	- 1761.57	3736.30	-45
45	5364.10	3736.57	- 1761.31	- 6094.23	-29115.46	-73510.96	-52004.36	2582.18	6345.70	2280.81	- 4613.85	- 8091.88	-28478.57	-53938.37	-19656.38	3556.98	45
0	-22127.42	-18966.05	-30253.34	-66397.49	-96564.11	-77686.97	-39101.51	-20050.32	-20352.12	-20049.75	-39102.79	-77686.88	-96562.81	-66398.24	-30253.42	-18966.63	0
0	-22127.42	-18966.05	-30253.34	-66397.49	-96564.11	-77686.97	-39101.51	-20050.32	-20352.12	-20049.75	-39102.79	-77686.88	-96562.81	-66398.24	-30253.42	-18966.63	0
0	-22127.42	-18966.05	-30253.34	-66397.49	-96564.11	-77686.97	-39101.51	-20050.32	-20352.12	-20049.75	-39102.79	-77686.88	-96562.81	-66398.24	-30253.42	-18966.63	0
45	5364.10	3736.57	- 1761.31	- 6094.23	-29115.46	-73510.96	-52004.36	2582.18	6345.70	2280.81	- 4613.85	- 8091.88	-28478.57	-53938.37	-19656.38	3556.98	45
-45	5364.10	3557.17	-19652.84	-53936.12	-28476.72	- 8092.01	- 4614.09	2280.54	6345.65	2582.49	-52001.54	-73506.98	-29113.79	- 6094.35	- 1761.57	3736.30	-45
0	-22127.42	-18966.05	-30253.34	-66397.49	-96564.11	-77686.97	-39101.51	-20050.32	-20352.12	-20049.75	-39102.79	-77686.88	-96562.81	-66398.24	-30253.42	-18966.63	0
0	-22127.42	-18966.05	-30253.34	-66397.49	-96564.11	-77686.97	-39101.51	-20050.32	-20352.12	-20049.75	-39102.79	-77686.88	-96562.81	-66398.24	-30253.42	-18966.63	0
-45	5364.10	3557.17	-19652.84	-53936.12	-28476.72	- 8092.01	- 4614.09	2280.54	6345.65	2582.49	-52001.54	-73506.98	-29113.79	- 6094.35	- 1761.57	3736.30	-45
45	5364.10	3736.57	- 1761.31	- 6094.23	-29115.46	-73510.96	-52004.36	2582.18	6345.70	2280.81	- 4613.85	- 8091.88	-28478.57	-53938.37	-19656.38	3556.98	45
θ \ J	1	2	3	4	5	6	7	8	9	10	11	12	13	14	15	16	J \ θ

Table 9. Maximum shear stresses around hole for various layers unstiffened composite panel (psi)

J / θ	1	2	3	4	5	6	7	8	9	10	11	12	13	14	15	16	J / θ
45	22594.13	14616.79	9608.73	9009.79	13747.17	36093.62	26169.03	8689.33	25896.12	15873.29	12604.30	9154.80	13432.71	26772.85	10539.98	17354.24	45
-45	22594.66	17355.40	10538.28	26771.73	13431.85	9155.70	12604.22	15872.73	25896.80	8690.28	26167.71	36091.61	13746.30	9010.27	9609.36	14616.52	-45
0	16621.70	13497.10	16034.71	33297.09	48739.50	38285.01	19416.14	13228.93	16420.06	13228.81	19416.96	38285.05	48738.79	33297.44	16034.64	13497.25	0
0	16621.70	13497.10	16034.71	33297.09	48739.50	38285.01	19416.14	13228.93	16420.06	13228.81	19416.96	38285.05	48738.79	33297.44	16034.64	13497.25	0
-45	22594.70	17355.40	10538.28	26771.73	13431.85	9155.70	12604.22	15872.73	25896.80	8690.28	26167.71	36091.61	13746.30	9010.27	9609.36	14616.52	-45
45	22594.10	14616.79	9608.73	9009.79	13747.17	36093.62	26169.03	8689.33	25896.12	15873.29	12604.30	9154.80	13432.71	26772.85	10539.98	17354.24	45
0	16621.70	13497.10	16034.71	33297.09	48739.50	38285.01	19416.14	13228.93	16420.06	13228.81	19416.96	38285.05	48738.79	33297.44	16034.64	13497.25	0
0	16621.70	13497.10	16034.71	33297.09	48739.50	38285.01	19416.14	13228.93	16420.06	13228.81	19416.96	38285.05	48738.79	33297.44	16034.64	13497.25	0
0	16621.70	13497.10	16034.71	33297.09	48739.50	38285.01	19416.14	13228.93	16420.06	13228.81	19416.96	38285.05	48738.79	33297.44	16034.64	13497.25	0
45	22594.10	14616.79	9608.73	9009.79	13747.17	36093.62	26169.03	8689.33	25896.12	15873.29	12604.30	9154.80	13432.71	26772.85	10539.98	17354.24	45
-45	22594.70	17355.40	10538.28	26771.73	13431.85	9155.70	12604.22	15872.73	25896.80	8690.28	26167.71	36091.61	13746.30	9010.27	9609.36	14616.52	-45
0	16621.70	13497.10	16034.71	33297.09	48739.50	38285.01	19416.14	13228.93	16420.06	13228.81	19416.96	38285.05	48738.79	33297.44	16034.64	13497.25	0
0	16621.70	13497.10	16034.71	33297.09	48739.50	38285.01	19416.14	13228.93	16420.06	13228.81	19416.96	38285.05	48738.79	33297.44	16034.64	13497.25	0
0	16621.70	13497.10	16034.71	33297.09	48739.50	38285.01	19416.14	13228.93	16420.06	13228.81	19416.96	38285.05	48738.79	33297.44	16034.64	13497.25	0
-45	22594.70	17355.40	10538.28	26771.73	13431.85	9155.70	12604.22	15872.73	25896.80	8690.28	26167.71	36091.61	13746.30	9010.27	9609.36	14616.52	-45
45	22594.10	14616.79	9608.73	9009.79	13747.17	36093.62	26169.03	8689.33	25896.12	15873.29	12604.30	9154.80	13432.71	26772.85	10539.98	17354.24	45
0	16621.70	13497.10	16034.71	33297.09	48739.50	38285.01	19416.14	13228.93	16420.06	13228.81	19416.96	38285.05	48738.79	33297.44	16034.64	13497.25	0
0	16621.70	13497.10	16034.71	33297.09	48739.50	38285.01	19416.14	13228.93	16420.06	13228.81	19416.96	38285.05	48738.79	33297.44	16034.64	13497.25	0
0	16621.70	13497.10	16034.71	33297.09	48739.50	38285.01	19416.14	13228.93	16420.06	13228.81	19416.96	38285.05	48738.79	33297.44	16034.64	13497.25	0
-45	22594.70	17355.40	10538.28	26771.73	13431.85	9155.70	12604.22	15872.73	25896.80	8690.28	26167.71	36091.61	13746.30	9010.27	9609.36	14616.52	-45
45	22594.10	14616.79	9608.73	9009.79	13747.17	36093.62	26169.03	8689.33	25896.12	15873.29	12604.30	9154.80	13432.71	26772.85	10539.98	17354.24	45
0	16621.70	13497.10	16034.71	33297.09	48739.50	38285.01	19416.14	13228.93	16420.06	13228.81	19416.96	38285.05	48738.79	33297.44	16034.64	13497.25	0
0	16621.70	13497.10	16034.71	33297.09	48739.50	38285.01	19416.14	13228.93	16420.06	13228.81	19416.96	38285.05	48738.79	33297.44	16034.64	13497.25	0
0	16621.70	13497.10	16034.71	33297.09	48739.50	38285.01	19416.14	13228.93	16420.06	13228.81	19416.96	38285.05	48738.79	33297.44	16034.64	13497.25	0
-45	22594.70	17355.40	10538.28	26771.73	13431.85	9155.70	12604.22	15872.73	25896.80	8690.28	26167.71	36091.61	13746.30	9010.27	9609.36	14616.52	-45
45	22594.10	14616.79	9608.73	9009.79	13747.17	36093.62	26169.03	8689.33	25896.12	15873.29	12604.30	9154.80	13432.71	26772.85	10539.98	17354.24	45
0	16621.70	13497.10	16034.71	33297.09	48739.50	38285.01	19416.14	13228.93	16420.06	13228.81	19416.96	38285.05	48738.79	33297.44	16034.64	13497.25	0
0	16621.70	13497.10	16034.71	33297.09	48739.50	38285.01	19416.14	13228.93	16420.06	13228.81	19416.96	38285.05	48738.79	33297.44	16034.64	13497.25	0
-45	22594.70	17355.40	10538.28	26771.73	13431.85	9155.70	12604.22	15872.73	25896.80	8690.28	26167.71	36091.61	13746.30	9010.27	9609.36	14616.52	-45
45	22594.10	14616.79	9608.73	9009.79	13747.17	36093.62	26169.03	8689.33	25896.12	15873.29	12604.30	9154.80	13432.71	26772.85	10539.98	17354.24	45
θ / J	1	2	3	4	5	6	7	8	9	10	11	12	13	14	15	16	θ / J

Table 10. Maximum principal stresses around hole for various layers of stiffened composite panel (psi)

J / θ	1	2	3	4	5	6	7	8	9	10	11	12	13	14	15	16	J / θ
45	65705.69	7923.13	7796.96	10285.85	-3005.99	-2414.02	50.59	4169.61	39395.81	37564.52	28539.46	19601.04	47.07	669.81	8366.82	72517.09	45
-45	62808.31	13541.08	- 790.46	-1468.61	-2805.72	2900.13	23227.09	32103.38	123783.05	59026.46	1210.99	-758.91	- 674.03	15221.10	32549.57	69968.01	-45
0	13275.34	3659.16	-1507.36	-1452.51	193.08	-1637.08	- 317.60	5023.76	16998.22	9993.14	283.39	-1140.60	1746.00	1547.57	5230.91	15093.48	0
0	13275.78	4230.42	-1177.84	-1301.32	271.95	-1612.37	- 293.04	5259.44	16865.83	9726.20	243.67	-1165.93	1669.51	1398.73	4889.74	14521.06	0
-45	63198.10	21406.30	- 225.22	-1218.41	-2558.62	4863.96	23919.78	32838.47	112306.75	49711.32	1056.22	- 971.97	- 972.01	14554.28	29216.45	61664.45	-45
45	65090.01	21045.87	12989.78	11322.07	-2489.63	-2049.80	298.76	8305.34	56624.92	36410.06	27386.09	15805.08	- 850.05	143.69	4011.86	59957.61	45
0	13277.17	5944.27	- 181.08	- 847.00	508.87	-1537.25	- 217.73	5969.63	16539.43	8938.14	133.78	-1240.33	1440.34	952.89	3868.54	12803.84	0
0	13277.67	6515.58	153.55	- 695.31	587.93	-1511.88	- 192.00	6207.53	16455.14	8679.08	99.60	-1264.64	1364.05	804.50	3529.00	12231.45	0
0	13278.17	7086.90	489.22	- 543.49	667.06	-1486.32	- 165.92	6446.06	16383.51	8421.60	66.41	-1288.70	1286.80	656.22	3189.93	11659.08	0
45	64597.65	31605.23	17185.73	12157.26	-2076.36	-1756.75	498.46	17058.62	70960.85	35492.20	26474.27	12823.47	-1409.47	- 242.18	2370.11	49910.06	45
-45	63978.02	37147.45	1028.52	- 697.79	-1986.25	9140.98	25324.96	34314.69	89422.54	31278.36	749.82	-1395.66	-1567.80	13226.69	22559.22	45061.81	-45
0	13279.76	8800.89	1501.87	- 87.27	904.70	-1408.53	- 85.12	7166.05	16245.96	7657.31	- 28.32	-1359.55	1059.35	212.09	2175.83	9942.06	0
0	13280.30	9372.24	1841.08	65.05	984.02	-1382.20	- 57.19	7407.69	16226.19	7404.93	- 58.54	-1382.73	983.30	64.27	1838.96	9369.76	0
0	13280.87	9943.59	2181.03	217.49	1063.38	-1355.67	- 28.70	7650.25	16219.48	7153.58	- 88.21	-1405.73	907.29	- 83.43	1502.73	8797.48	0
-45	64498.23	47643.87	2066.46	- 330.74	-1522.84	12518.94	26275.68	35303.39	74258.13	19453.31	547.41	-1676.29	-1964.85	12346.39	18131.55	34000.22	-45
45	63859.48	47461.61	23514.58	13419.74	-1456.19	-1314.50	800.42	33931.77	92773.43	34124.64	25125.62	8495.06	-2078.21	- 781.46	798.03	34838.92	45
0	13282.64	11657.64	3204.86	675.62	1301.79	-1274.75	60.96	8384.24	16276.99	6405.09	- 174.37	-1473.55	679.54	- 525.86	498.41	7080.84	0
0	13283.26	12228.99	3547.33	828.58	1381.37	-1247.31	92.51	8631.29	16321.56	6157.23	- 202.27	-1495.79	603.72	- 673.12	165.28	6508.71	0
0	13283.88	12800.35	3890.34	981.68	1461.00	-1219.62	125.09	8879.73	16378.51	5910.10	- 229.84	-1517.87	527.93	- 820.26	- 166.94	5936.63	0
45	63367.60	58036.75	27747.44	14267.49	-1042.58	-1017.89	1003.71	45668.78	107409.94	33218.93	24239.86	5759.28	-2446.59	-1121.97	- 42.14	24791.75	45
-45	65278.90	63389.70	4933.25	264.27	- 633.38	16832.33	27721.45	36793.37	51861.91	6529.38	245.95	-2094.43	-2560.22	11033.68	11520.49	17444.27	-45
0	13285.84	14514.44	4899.18	1441.73	1700.20	-1135.01	230.36	9634.61	16620.80	5172.60	- 310.69	-1583.12	300.85	-1261.01	-1157.33	4220.86	0
0	13286.52	15085.80	5196.88	1595.33	1780.05	-1106.25	268.63	9889.94	16724.34	4927.93	-337.13	-1604.56	225.24	-1407.71	-1485.06	3649.15	0
-45	65669.39	71262.90	7297.63	590.29	- 58.99	19213.01	28452.71	37541.56	41082.48	4393.91	96.01	-2302.21	-2857.80	10381.04	8241.16	9246.20	-45
45	62753.03	71257.80	33748.91	15333.60	- 525.38	- 645.20	1260.68	60486.85	125760.12	32093.30	23148.46	2612.87	-2847.71	-1532.09	- 996.45	12233.99	45
θ / J	1	2	3	4	5	6	7	8	9	10	11	12	13	14	15	16	θ / J

Table 11. Minimum principal stresses around hole for various layers of stiffened composite panel (psi)

J / θ	1	2	3	4	5	6	7	8	9	10	11	12	13	14	15	16	J / θ
45	7218.7	612.7	- 4780.0	- 8302.1	- 31355.4	-80575.4	-69407.8	-13698.0	10744.1	5972.2	- 3659.9	- 7969.4	- 20678.2	-42615.5	- 2770.0	7540.7	45
-45	7350.1	912.6	-48863.0	-77257.2	- 41975.5	-10585.5	- 6375.9	- 633.2	7479.2	4806.5	-47431.2	-81316.9	- 31285.0	- 5418.8	185.0	7252.0	-45
0	-13679.0	-14104.1	-28440.3	-74368.5	-108314.8	-93203.2	-57670.8	-38323.9	-6021.8	-15947.6	-27875.4	-74945.8	-101276.3	-70600.3	-36981.8	-34408.5	0
0	-13676.8	-15119.7	-28854.8	-74175.4	-107959.7	-92287.0	-56182.1	-37210.7	-5932.6	-17066.0	-29361.5	-75852.8	-101622.1	-70782.3	-36544.7	-33393.3	0
-45	7334.8	1775.6	-42067.8	-72601.4	- 39003.1	- 9937.7	- 6006.4	219.2	8099.1	4325.3	-50361.9	-81213.6	- 31300.0	- 5780.4	- 430.2	6408.5	-45
45	7250.2	2135.2	- 3621.2	- 7651.8	- 31352.5	-80732.2	-64725.8	- 2222.9	10734.1	4522.9	- 4229.9	- 8288.5	- 24922.9	-49917.7	-10197.9	6090.7	45
0	-13670.2	-18166.5	-30106.3	-73596.7	-106894.9	-89539.2	-51717.9	-33874.1	-5735.8	-20433.9	-33829.0	-78575.4	-102659.9	-71328.9	-35235.6	-30347.6	0
0	-13668.0	-19182.1	-30525.9	-73404.0	-106540.1	-88623.7	-50230.4	-32763.1	-5694.7	-21560.2	-35320.6	-79483.4	-103006.0	-71511.3	-34800.1	-29332.4	0
0	-13665.9	-20197.7	-30946.5	-73211.5	-106185.3	-87708.3	-48743.3	-31652.7	-5666.3	-22688.0	-36813.2	-80391.7	-103352.0	-71693.8	-34365.0	-28317.2	0
45	7275.2	3292.0	- 2735.8	- 7137.8	- 31350.4	-80859.2	-60981.4	1512.5	10173.4	3357.7	- 4696.8	- 8599.0	- 28476.9	-55794.5	-17982.4	4930.7	45
-45	7303.8	3490.8	-28600.8	-63310.2	- 33136.6	- 9099.5	- 5287.1	1917.9	9270.5	3165.5	-56226.5	-81009.3	- 31330.1	- 6509.7	- 1669.5	4717.0	-45
0	-13659.5	-23244.7	-32213.9	-72634.7	-105121.2	-84963.2	-44284.6	-28325.9	-5658.4	-26079.7	-41295.8	-83117.8	-104390.6	-72242.1	-33063.0	-25271.7	0
0	-13657.4	-24260.3	-32638.0	-72442.7	-104766.6	-84048.6	-42799.3	-27218.6	-5681.8	-27212.7	-42791.4	-84026.9	-104736.8	-72425.1	-32630.2	-24256.6	0
0	-13655.3	-25276.0	-33062.9	-72250.8	-104412.0	-83134.2	-41314.6	-26112.2	-5718.3	-28346.7	-44287.5	-84936.3	-105083.1	-72608.2	-32198.0	-23241.5	0
-45	7282.9	4632.0	-19824.9	-57136.1	- 29307.5	- 8683.3	- 4821.5	3045.8	9959.7	1928.7	-60138.1	-80875.0	- 31350.3	- 7000.6	- 2506.2	3582.5	-45
45	7312.4	5009.9	- 1442.6	- 6376.5	- 31347.5	-81052.6	-55367.3	3372.3	9023.7	1600.8	- 5416.2	- 9208.7	- 33978.5	-64649.2	-30549.8	3190.5	45
0	-13649.1	-28323.0	-34341.5	-71676.0	-103348.7	-80392.2	-36864.7	-22799.4	-5905.4	-31754.2	-48778.7	-87665.4	-106122.3	-73158.2	-30905.8	-20196.4	0
0	-13647.0	-29338.7	-34768.9	-71484.6	-102994.4	-79478.7	-35383.1	-21697.6	-5993.2	-32891.7	-50276.6	-88575.5	-106468.8	-73341.7	-30476.6	-19181.4	0
0	-13645.0	-30354.4	-35196.8	-71293.3	-102640.1	-78565.5	-33902.5	-20597.1	-6093.4	-34029.8	-51774.8	-89485.8	-106815.4	-73525.4	-30048.5	-18166.5	0
45	7336.9	6151.0	- 594.1	- 5875.0	- 31345.8	-81183.2	-51626.5	4123.9	8162.4	423.5	- 5909.2	- 9765.0	- 37723.6	-70571.4	-39135.9	2030.0	45
-45	7251.2	6342.6	- 6584.0	-47919.3	- 23758.1	- 8205.5	- 4142.8	4730.7	10643.1	- 4740.2	-66007.5	-80676.4	- 31380.9	- 7744.7	- 3791.7	1844.3	-45
0	-13638.9	-33401.4	-34204.8	-70720.4	-101577.5	-75827.2	-29468.2	-17305.2	-6465.3	-37448.3	-56271.3	-92217.5	-107855.3	-74077.1	-28770.1	-15122.3	0
0	-13637.0	-34417.1	-34464.8	-70529.7	-101223.5	-74915.0	-27993.3	-16211.6	-6612.0	-38589.0	-57770.6	-93128.4	-108202.0	-74261.2	-28346.5	-14107.7	0
-45	7235.2	7197.6	- 3163.9	-43339.4	- 21113.1	- 8010.6	- 3811.8	5570.0	10566.1	-12401.1	-68943.1	-80578.3	- 31396.3	- 8120.5	- 4460.7	895.3	-45
45	7367.3	7575.2	525.7	- 5254.6	- 31343.8	-81348.5	-46953.3	4916.6	7031.2	- 1054.7	- 6541.2	-10733.7	- 42464.3	-77989.6	-49964.4	578.3	45
θ / J	1	2	3	4	5	6	7	8	9	10	11	12	13	14	15	16	θ / J

Table 12. Maximum shear stresses around hole for various layers stiffened composite panel (psi)

θ \ J	1	2	3	4	5	6	7	8	9	10	11	12	13	14	15	16	J \ θ
45	29243.5	3655.2	6288.5	9294.0	14174.7	39080.7	34729.2	8933.8	14325.8	15796.2	16099.7	13785.2	10362.6	21642.6	5568.4	32488.2	45
-45	27729.1	6314.2	24036.3	37894.3	19584.8	6742.8	14801.5	16368.3	58151.9	27110.0	24321.1	40279.0	15305.5	10319.9	16182.3	31358.0	-45
0	13477.2	8881.6	13466.5	36458.0	54253.9	45783.1	28676.6	21673.8	11510.0	12970.4	14079.4	36902.6	51511.2	36074.0	21106.4	24751.0	0
0	13476.3	9675.0	13838.5	36437.0	54115.8	45337.3	27944.5	21235.1	11399.2	13396.1	14802.6	37343.4	51645.8	36090.5	20717.2	23957.2	0
-45	27931.6	9815.4	20921.3	35691.5	18222.2	7418.8	14963.1	16309.7	52103.8	22693.0	25709.1	40120.8	15164.0	10167.3	14823.3	27628.0	-45
45	28919.9	9455.4	8305.5	9486.9	14431.5	39341.2	32512.3	5264.1	22945.4	15943.6	15808.0	12046.8	12036.4	25030.7	7104.9	26933.5	45
0	13473.7	12055.4	14962.6	36374.8	53701.9	44001.0	25750.1	19921.9	11137.6	14686.0	16981.4	38667.5	52050.1	36140.9	19552.1	21575.7	0
0	13472.9	12848.8	15339.7	36354.4	53564.0	43555.9	25019.2	19485.3	11074.9	15119.6	17710.1	39109.4	52185.0	36157.9	19164.5	20781.9	0
0	13472.0	13642.3	15717.8	36334.0	53426.2	43111.0	24288.7	19049.4	11024.9	15554.8	18439.8	39551.5	52320.0	36175.0	18777.5	19988.1	0
45	28661.2	14156.6	9960.7	9647.5	14637.0	39551.3	30739.9	7773.1	30393.7	16067.2	15585.5	10711.2	13533.7	27776.2	10176.3	22489.7	45
-45	28337.1	16828.3	14814.7	31306.2	15575.2	9120.3	15306.0	16198.4	40076.0	14056.5	28488.2	39806.8	14881.2	9868.2	12114.4	20172.4	-45
0	13469.6	16022.8	16857.9	36273.7	53012.9	41777.3	22099.7	17746.0	10952.2	16868.5	20633.7	40879.1	52725.0	36227.1	17619.4	17606.9	0
0	13468.8	16816.3	17239.6	36253.9	52875.3	41333.2	21371.1	16313.1	10954.0	16738.8	21366.4	41322.1	52860.1	36244.7	17234.6	16813.2	0
0	13468.1	17609.8	17622.0	36234.2	52737.7	40889.2	20643.0	16881.2	10968.9	17750.1	22099.6	41765.3	52995.2	36262.4	16850.4	16019.5	0
-45	28607.7	21505.9	10945.7	28402.7	13892.3	10421.1	15548.6	16128.8	32149.2	8762.3	30342.7	39599.4	14692.7	9673.5	10318.9	15208.9	-45
45	28273.6	21225.8	12478.6	9898.1	14945.7	39869.0	28083.8	15279.8	41874.9	16261.9	15270.9	8851.9	15950.1	31933.9	15673.9	15824.2	45
0	13465.9	19990.3	18773.2	36175.8	52325.2	39558.7	18462.9	15591.8	11091.2	19079.6	24302.2	43095.9	53400.9	36316.2	15702.1	13638.6	0
0	13465.1	20783.8	19158.1	36156.6	52187.9	39115.7	17737.8	15164.4	11157.4	19524.4	25037.2	43539.9	53536.3	36334.3	15321.0	12845.1	0
0	13464.4	21577.4	19543.6	36137.5	52050.5	38672.9	17013.8	14738.4	11235.9	19970.0	25772.5	43983.9	53671.7	36352.6	14940.8	12051.6	0
45	28015.3	25942.9	14170.8	10071.3	15151.6	40082.7	26315.1	20772.4	49623.8	16397.7	15074.5	7762.2	17638.5	34724.7	19546.9	11380.9	45
-45	29013.9	28523.6	5758.6	24091.8	11562.4	12518.9	15932.1	16031.3	20609.4	5634.8	33126.8	39291.0	14410.4	9389.2	7656.1	7800.0	-45
0	13462.4	23957.9	19552.0	36081.1	51638.9	37346.1	14849.3	13469.9	11543.0	21310.5	27980.3	45317.2	54078.1	36408.0	13806.4	9671.6	0
0	13461.7	24751.4	19830.8	36062.5	51501.8	36904.4	14131.0	13050.8	11668.2	21758.5	28716.8	45761.9	54213.6	36426.7	13430.7	8878.5	0
-45	29217.1	32032.7	5230.8	21964.9	10527.1	13611.8	16132.2	15985.8	15258.2	8397.5	34519.6	39138.1	14269.2	9250.8	6350.9	4175.5	-45
45	27692.9	31841.3	16611.7	10294.1	15409.2	40351.6	24107.0	27785.1	59364.4	16574.0	14844.8	6673.3	19808.3	38228.8	24484.0	5827.8	45
θ \ J	1	2	3	4	5	6	7	8	9	10	11	12	13	14	15	16	J \ θ

Table 13. Effect of Stiffeners on Stress Concentration Factor for Aluminum Panels with hole based on Global Analysis

Case	Panel Type	Far Field Stress (psi)	Stress Concentration Factor
1		32443.20	2.74
2	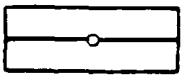	32187.60	2.93
3	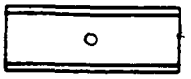	32763.90	2.69
4	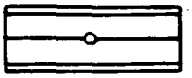	32994.29	2.89

Table 14. Effect of Stiffeners on Dimensionless Maximum Stress Resultants for Composite Panels with hole based on Global Analysis

Case	PanelType	Far Field Stress Resultant (ppi)	Dimensionless Maximum Stress Resultant
1		4906.32	1.74
2	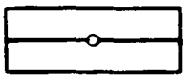	4891.76	1.84
3		5143.22	1.66
4	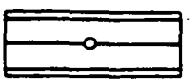	5127.40	1.80

Table 15. Computational Times and Speedups for Unstiffened and Stiffened Aluminum Panels with Hole

Number of Processors	Computational Time (seconds)		Speedup	
	Unstiffened	Stiffened	Unstiffened	Stiffened
1	22.2	684.0	-	-
2	11.4	346.0	1.9	2.0
4	6.2	179.0	3.6	3.8
8	4.3	92.3	5.1	7.4
16	4.1	50.5	5.4	13.5

Table 16. Computational Times and speedups for Aluminum Panel with Hole and Inner Stiffener (I.S.) or Outer Stiffener(O.S.)

Number of Processors	Computational Time (seconds)		Speedup	
	with I.S.	with O.S.	with I.S.	with O.S.
1	408.0	486.0	-	-
2	206.0	245.0	2.0	2.0
4	106.0	127.0	3.8	3.8
8	55.7	65.7	7.3	7.4
16	31.6	36.6	12.96	13.3

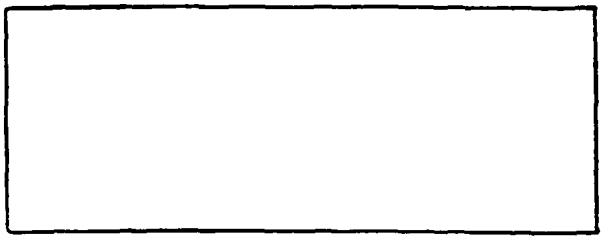

(a) Rectangular Panel

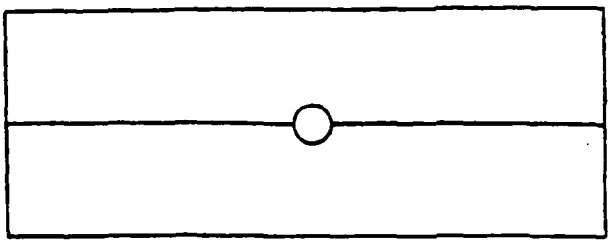

(d) Panel with Inner Stiffener

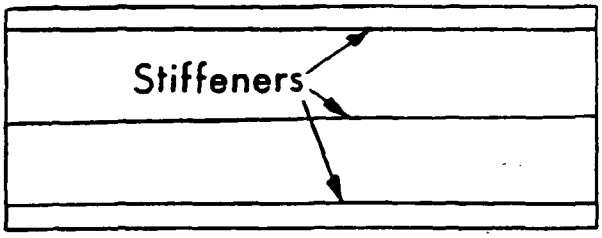

(b) Panel with Stiffeners

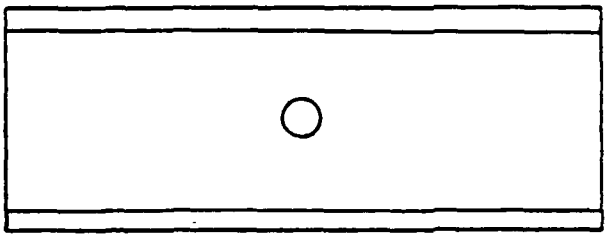

(e) Panel with Outer Stiffener

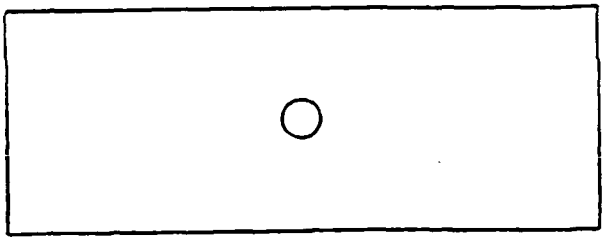

(c) Unstiffened Panel with Hole

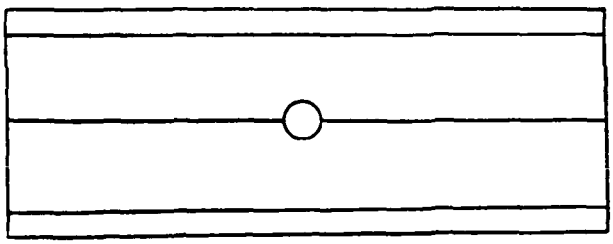

(f) Stiffened Panel with Hole

Figure 1. Types of panels

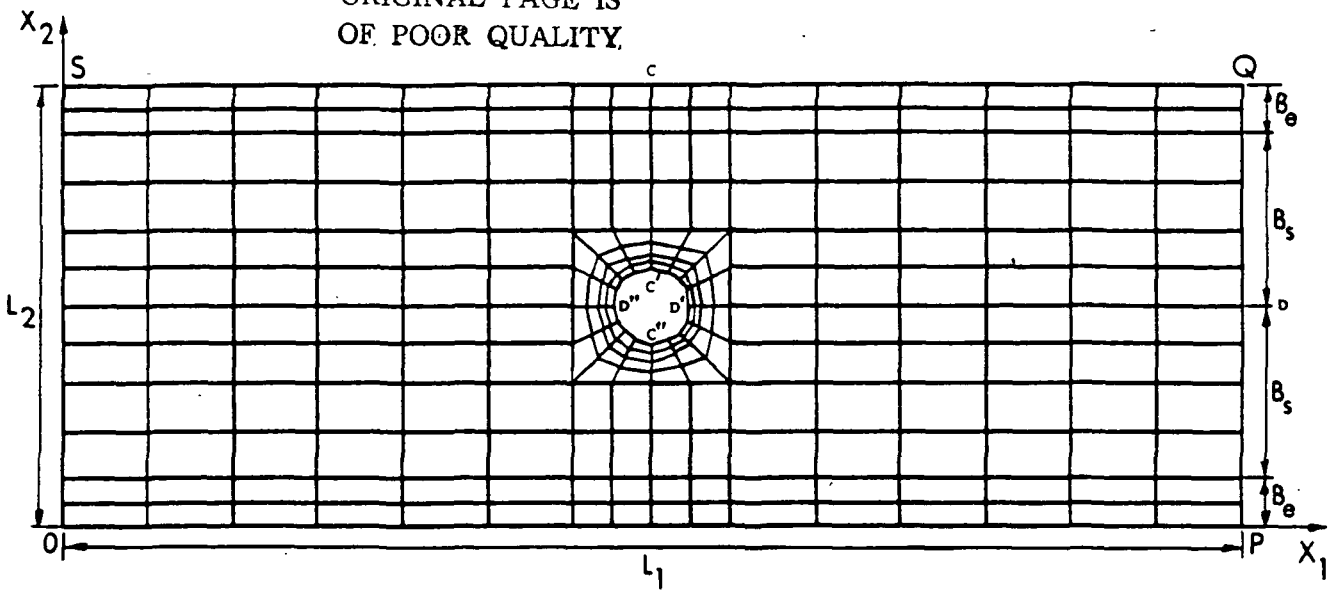

(a) Global Discretization for Panel Skin

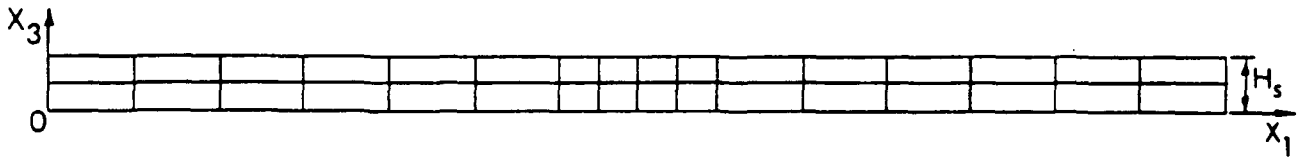

(b) Stiffener Discretization

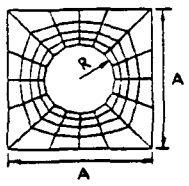

(c) Discretization Around Hole

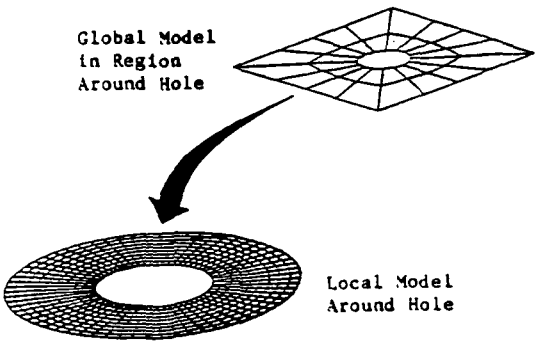

(d) Global/Local Discretization Around Hole

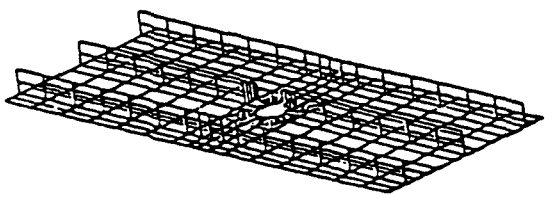

(e) Discretization for Stiffened Panel with Hole

Figure 2. Finite Element Discretizations

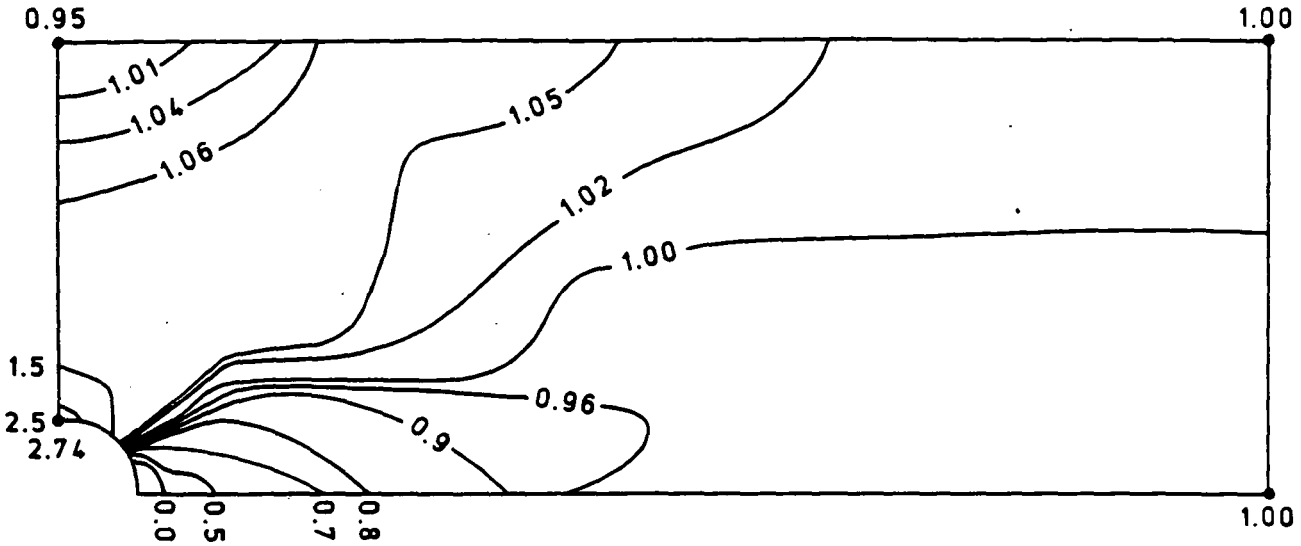

(a) By global analysis

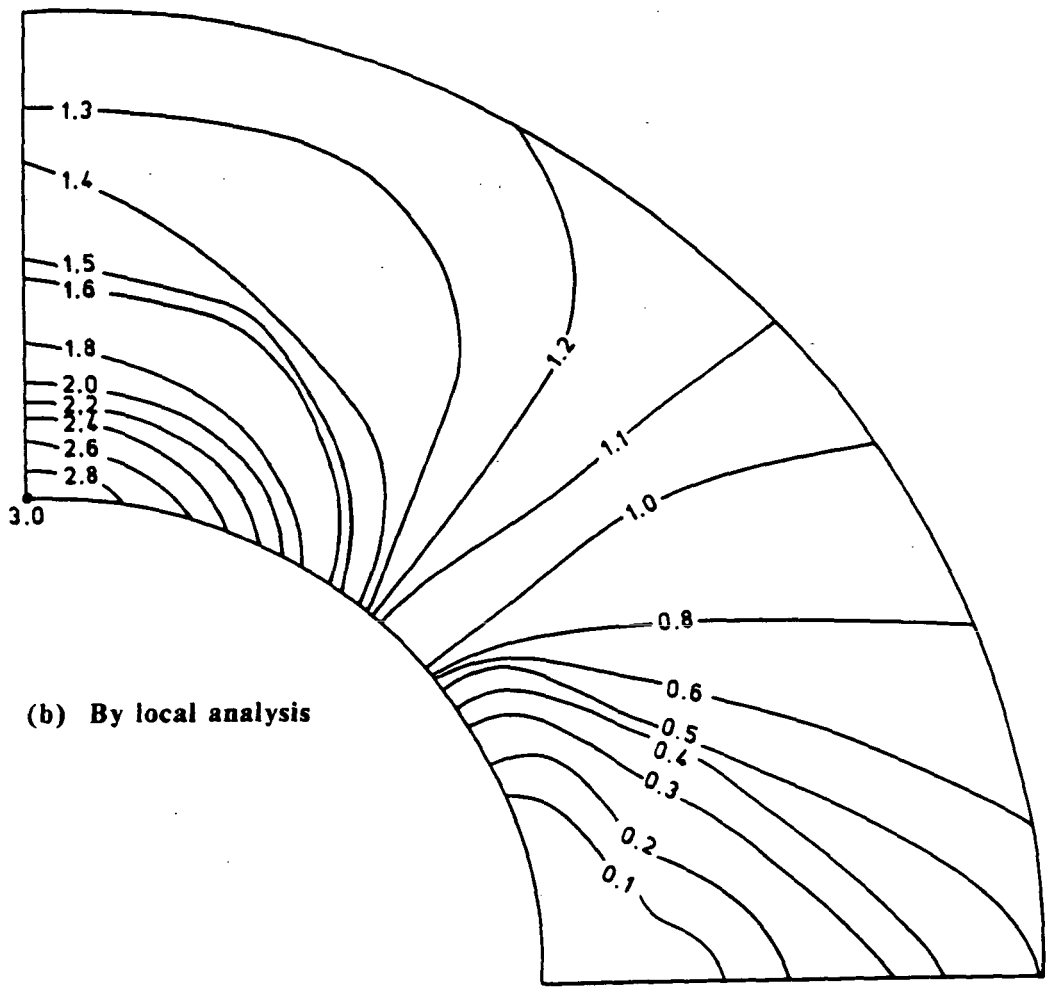

(b) By local analysis

Figure 3. Contours for dimensionless compressive principal stress for unstiffened aluminum panel with hole (σ_0 = 32443.20 psi)

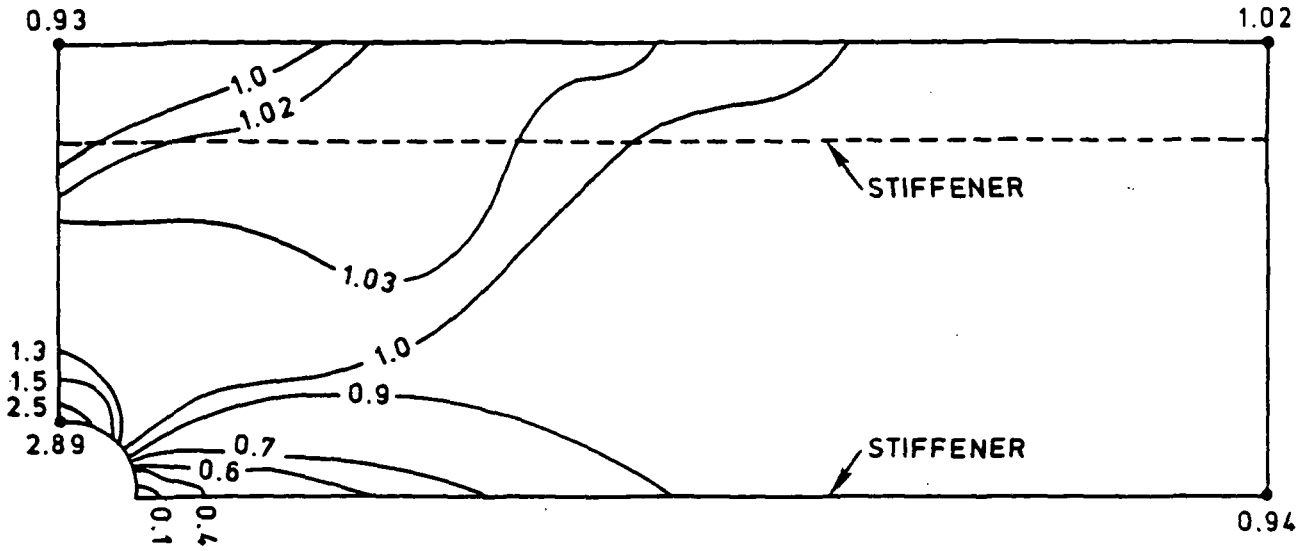

(a) Panel skin

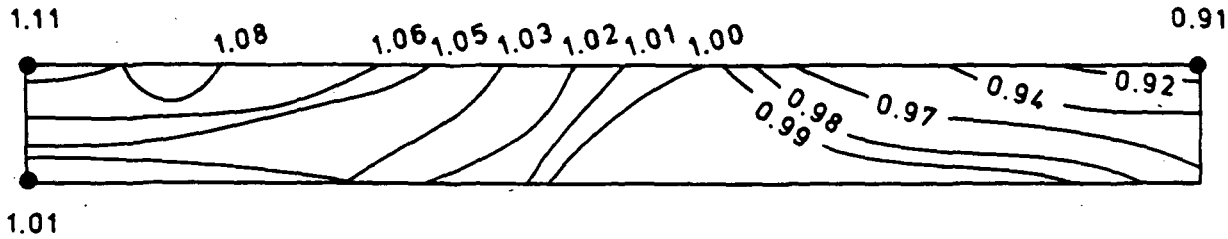

(b) Outer stiffener

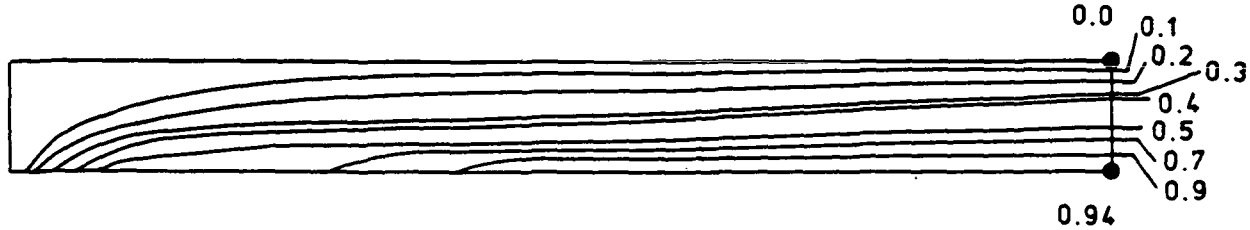

(c) Inner stiffener

Figure 4. Contours for dimensionless compressive principal stress for stiffened aluminum panel by global analysis (σ_0 = 32994.29 psi)

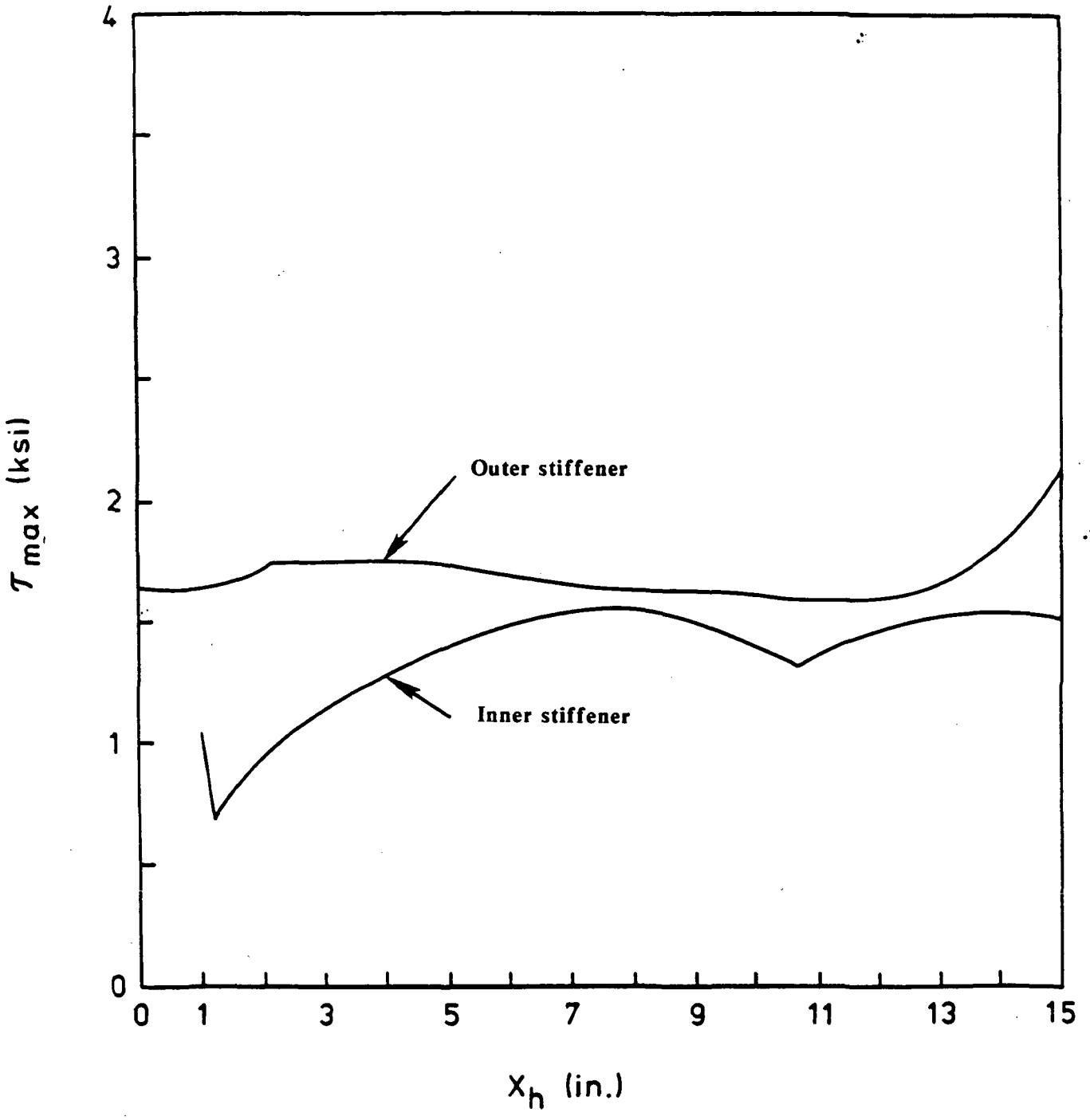

Figure 5. Midsurface maximum shear stress distribution for aluminum panel at location of stiffeners

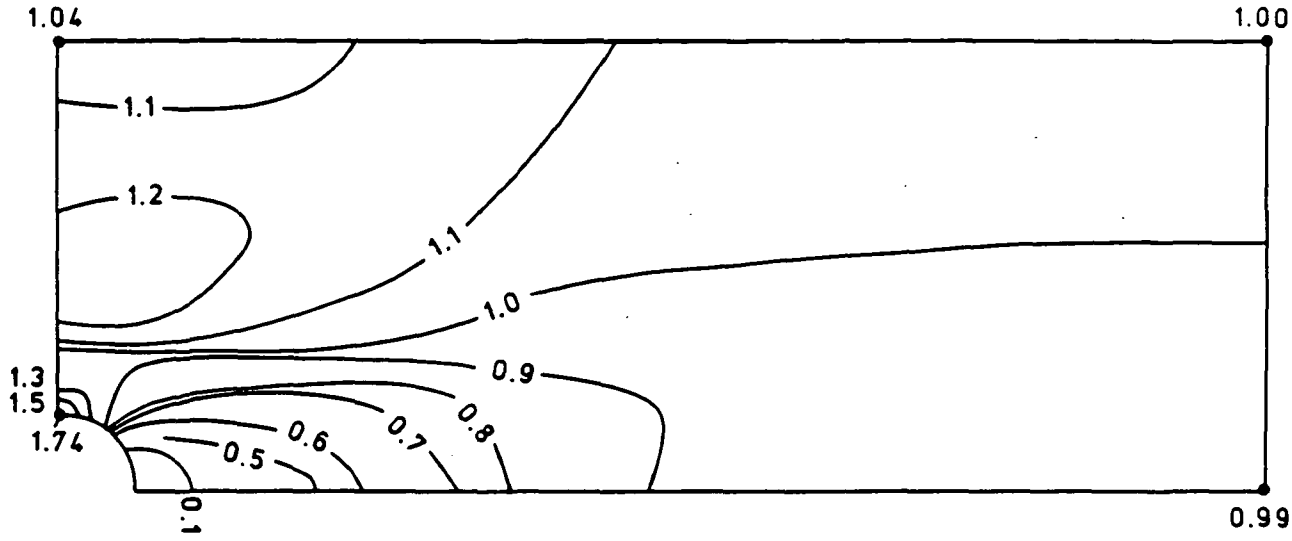

(a) By global analysis

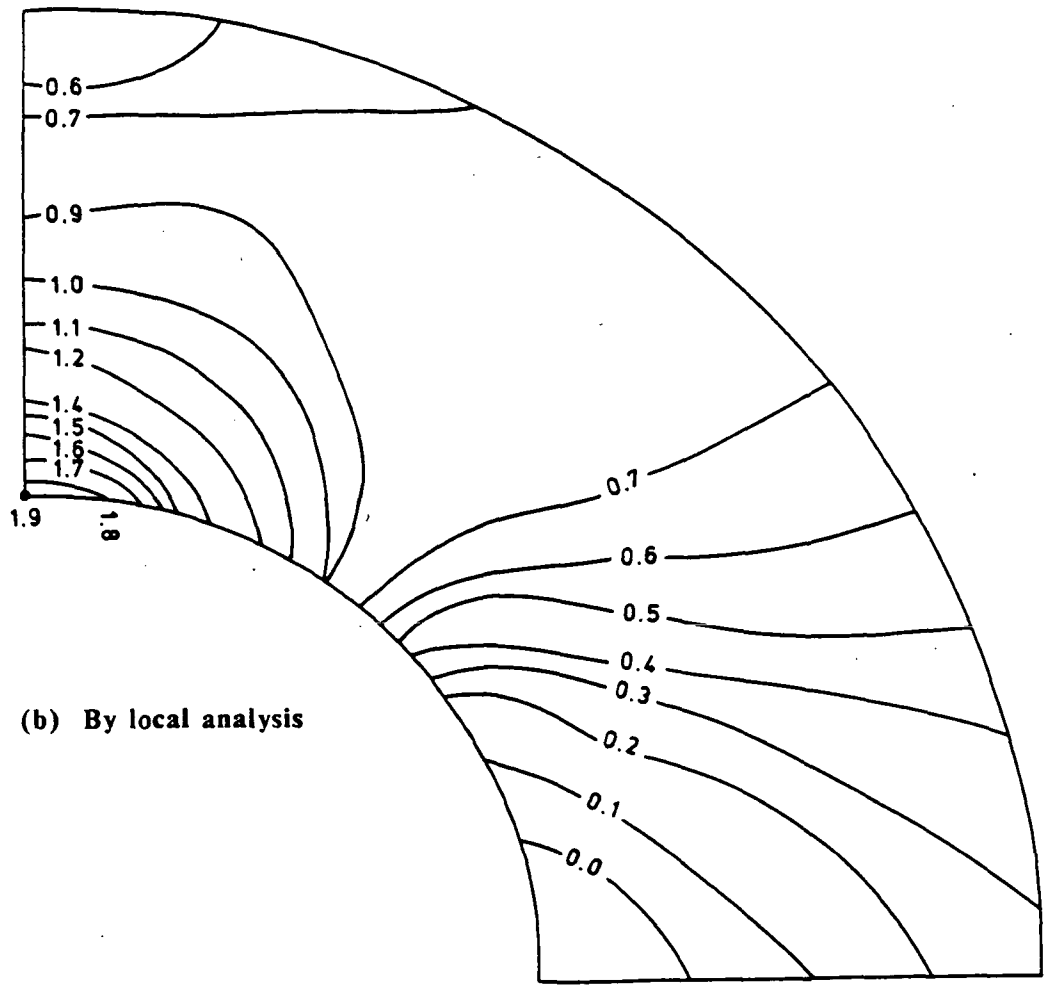

(b) By local analysis

Figure 6. Contours for dimensionless compressive principal stress resultants for unstiffened composite panel with hole (σ_o = 4906.32 ppi)

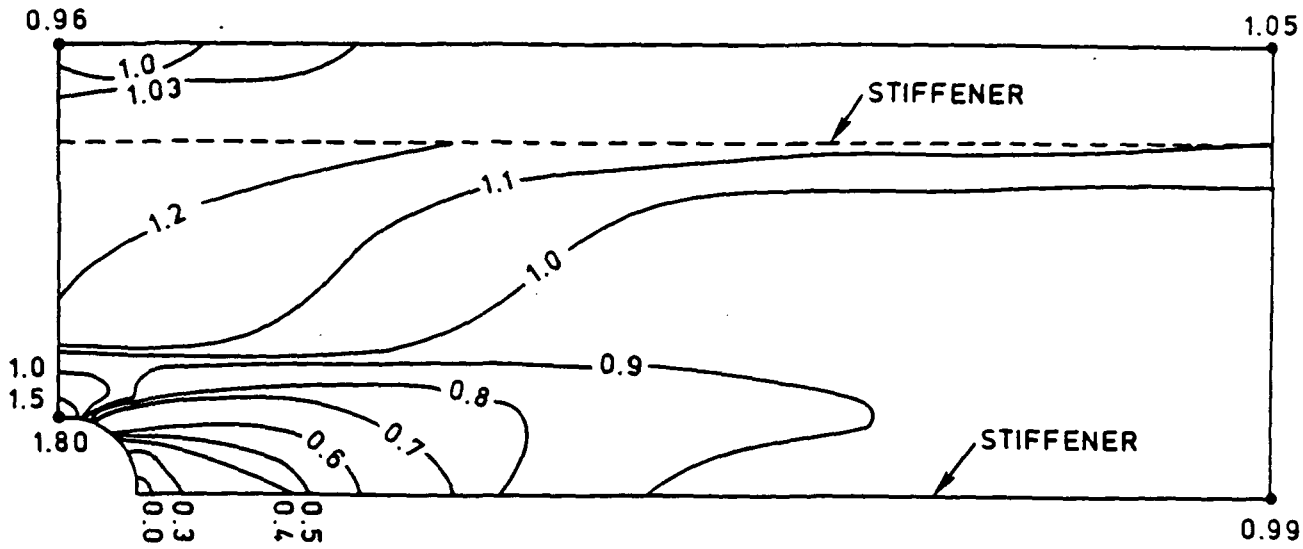

(a) Panel skin

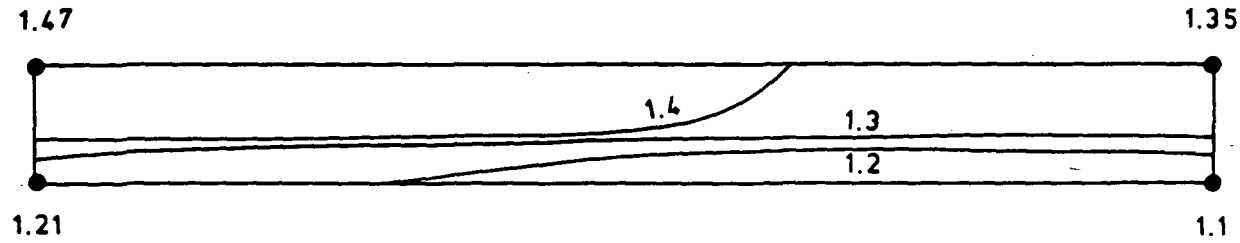

(b) Outer stiffener

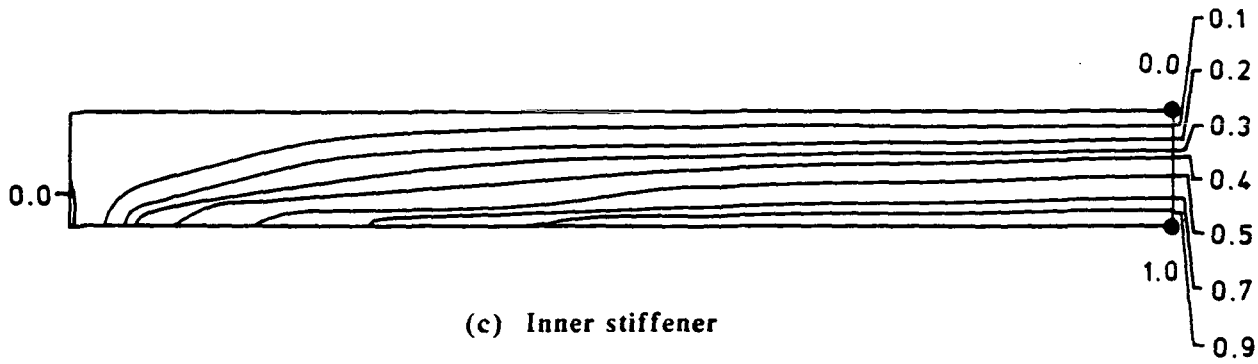

(c) Inner stiffener

Figure 7. Contours for dimensionless compressive principal stress resultants for stiffened composite panel by global analysis (σ_0 = 5127.40 ppi)

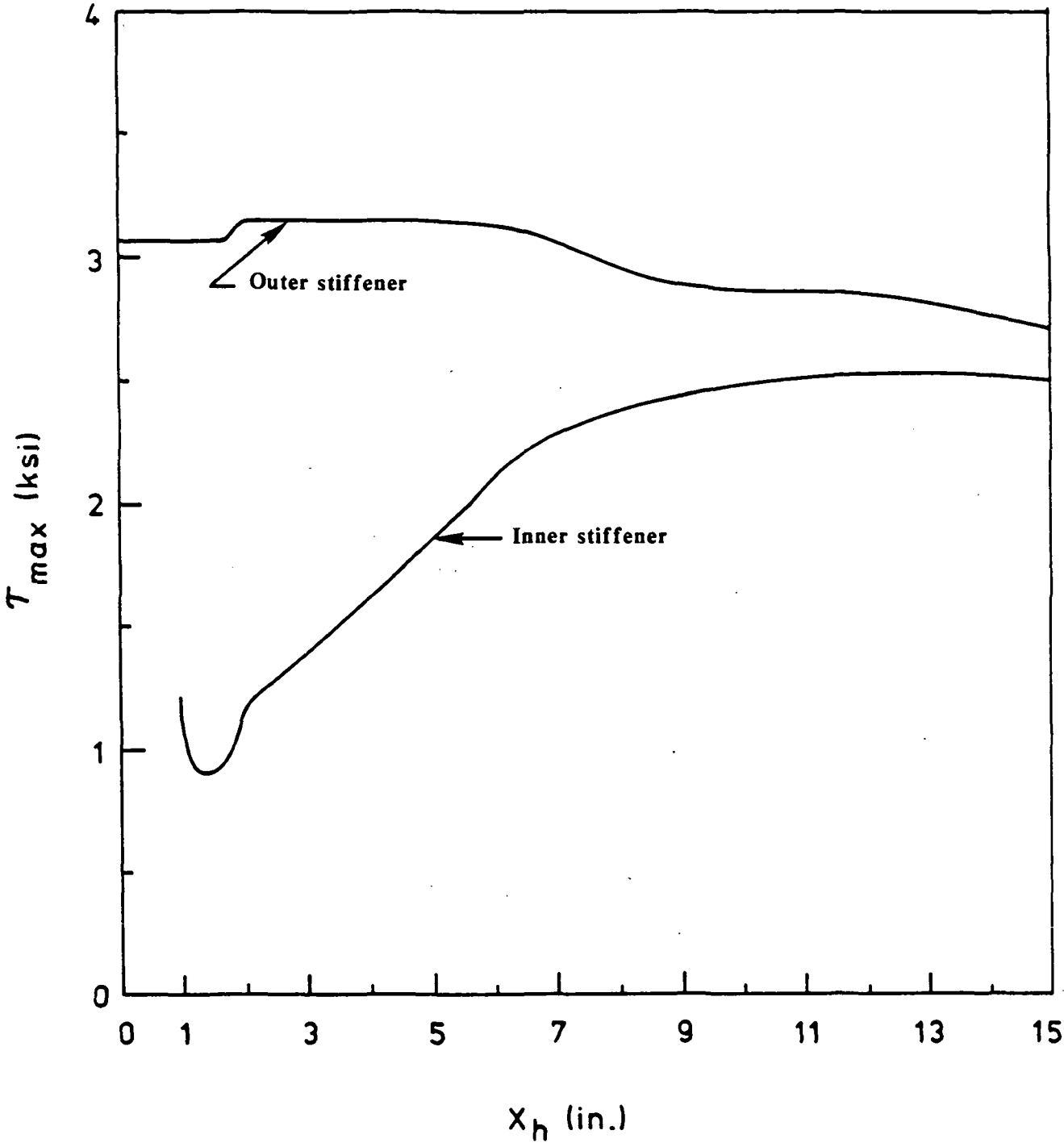

Figure 8. Distribution of maximum shear stress resultants for composite panel at location of stiffeners

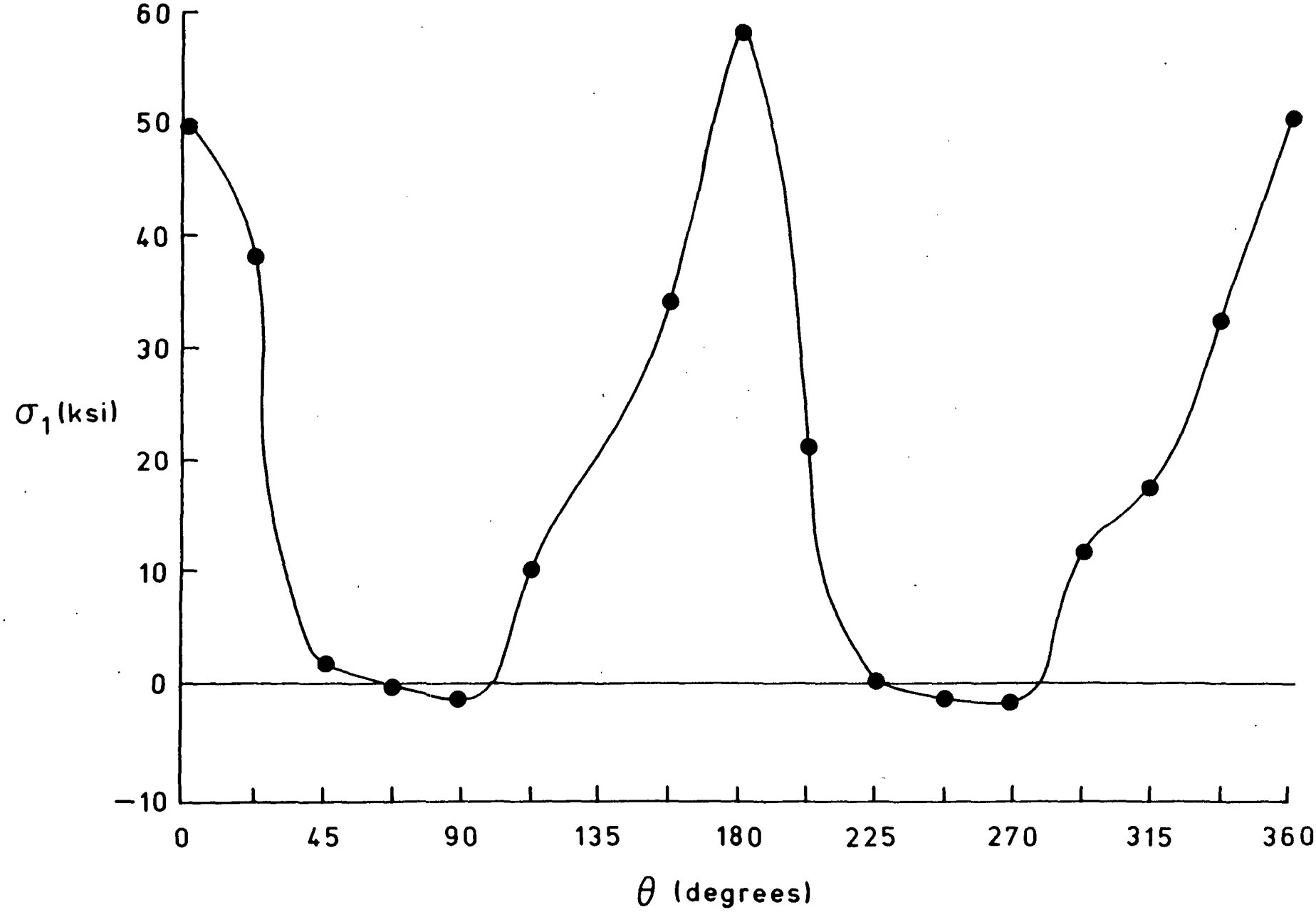

Figure 9. Maximum principal stresses around hole for -45° ply-orientation for unstiffened composite panel

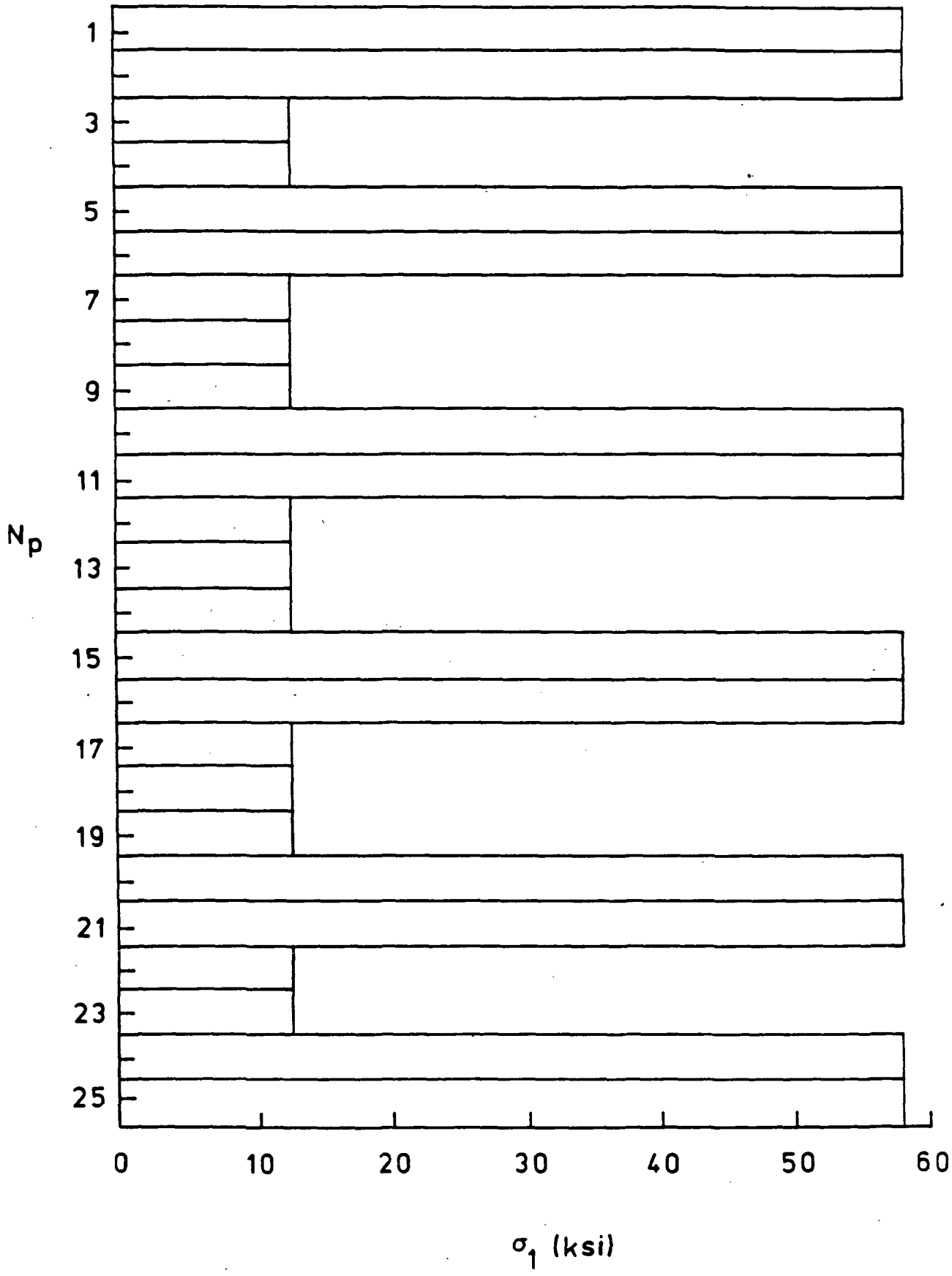

Figure 10. Maximum principal stresses for various layers of unstiffened composite panel

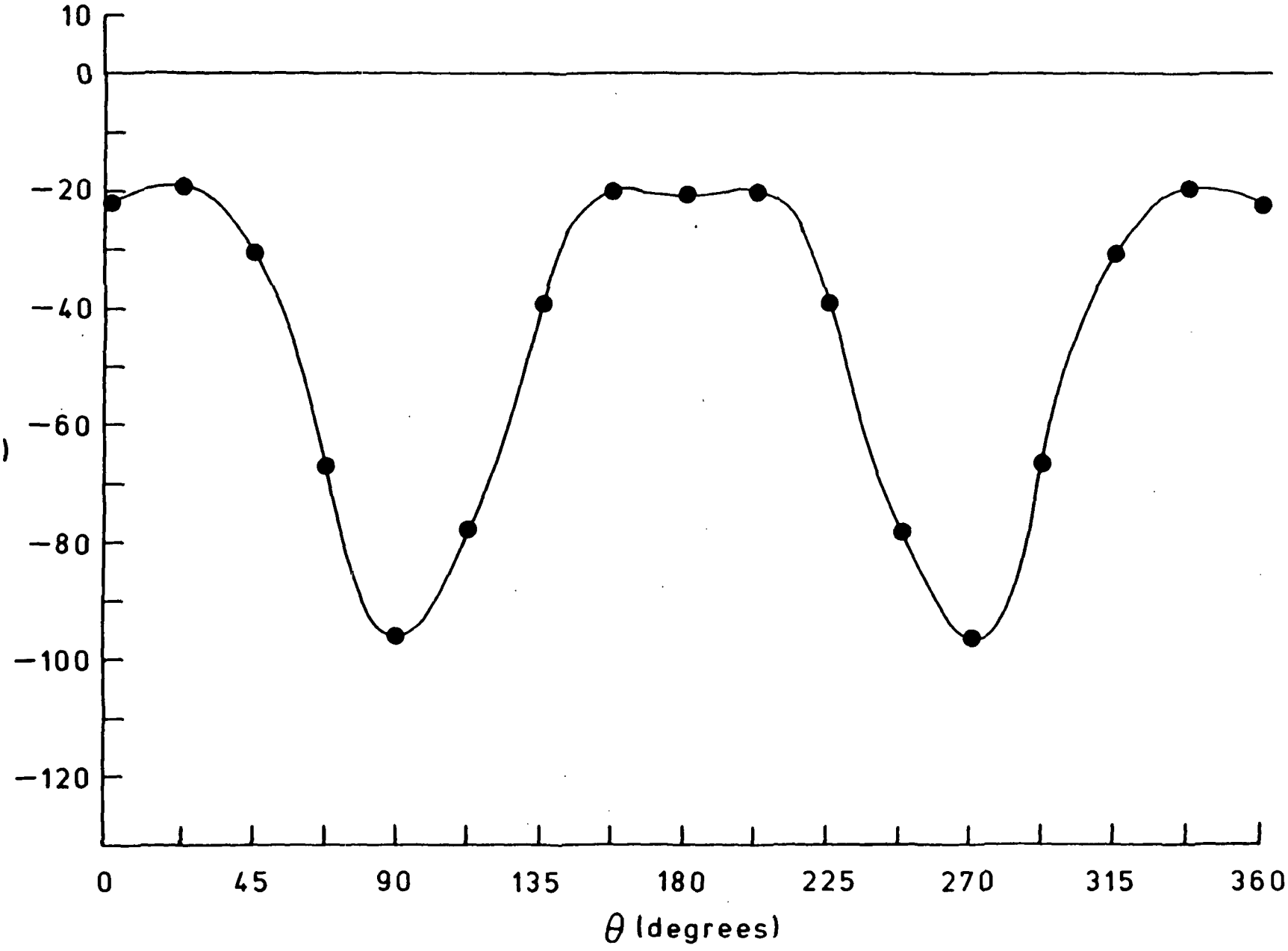

Figure 11. Minimum principal stresses around hole for 0^o ply-orientation for unstiffened composite panel

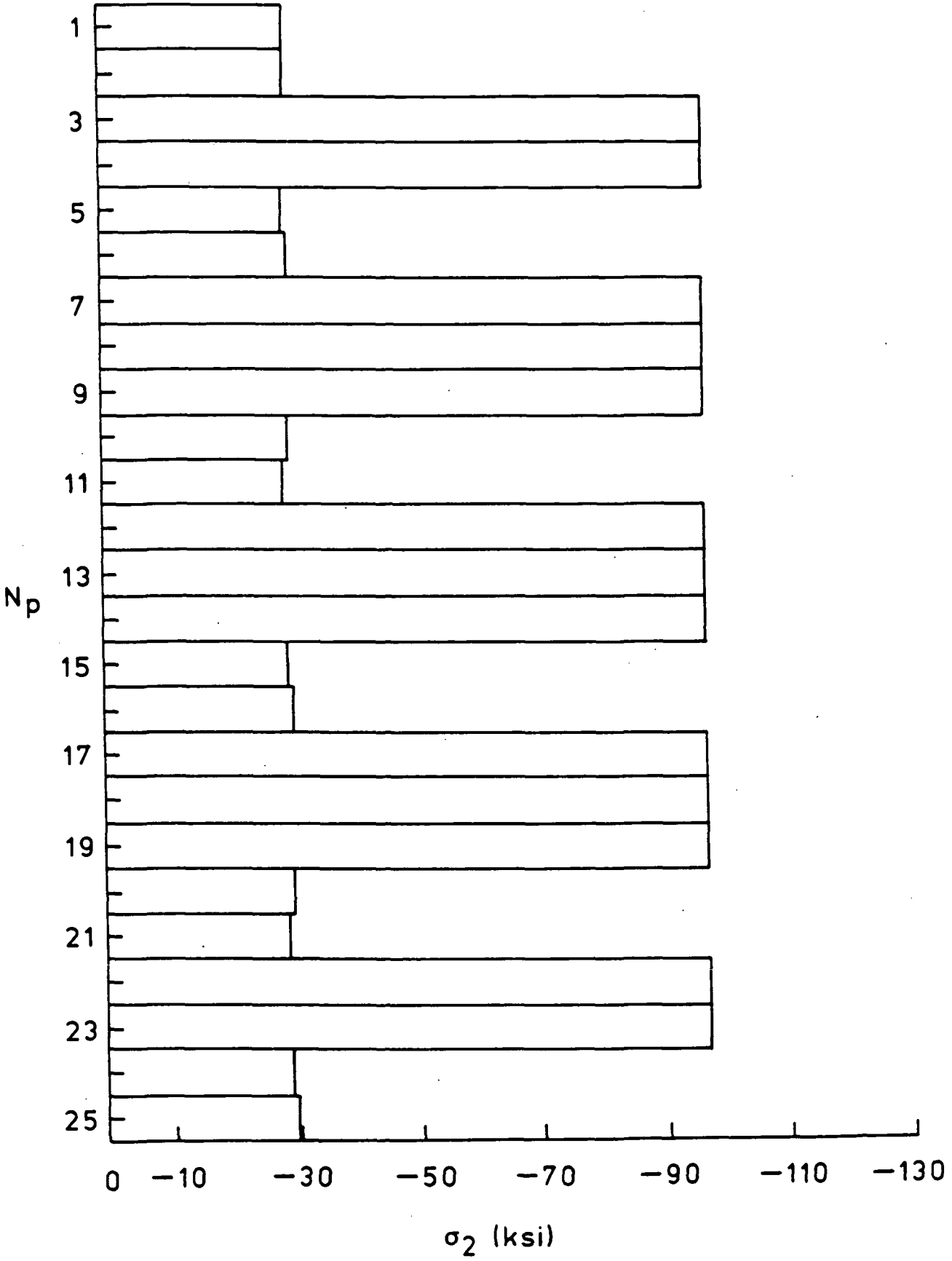

Figure 12. Minimum principal stresses for various layers of unstiffened composite panel

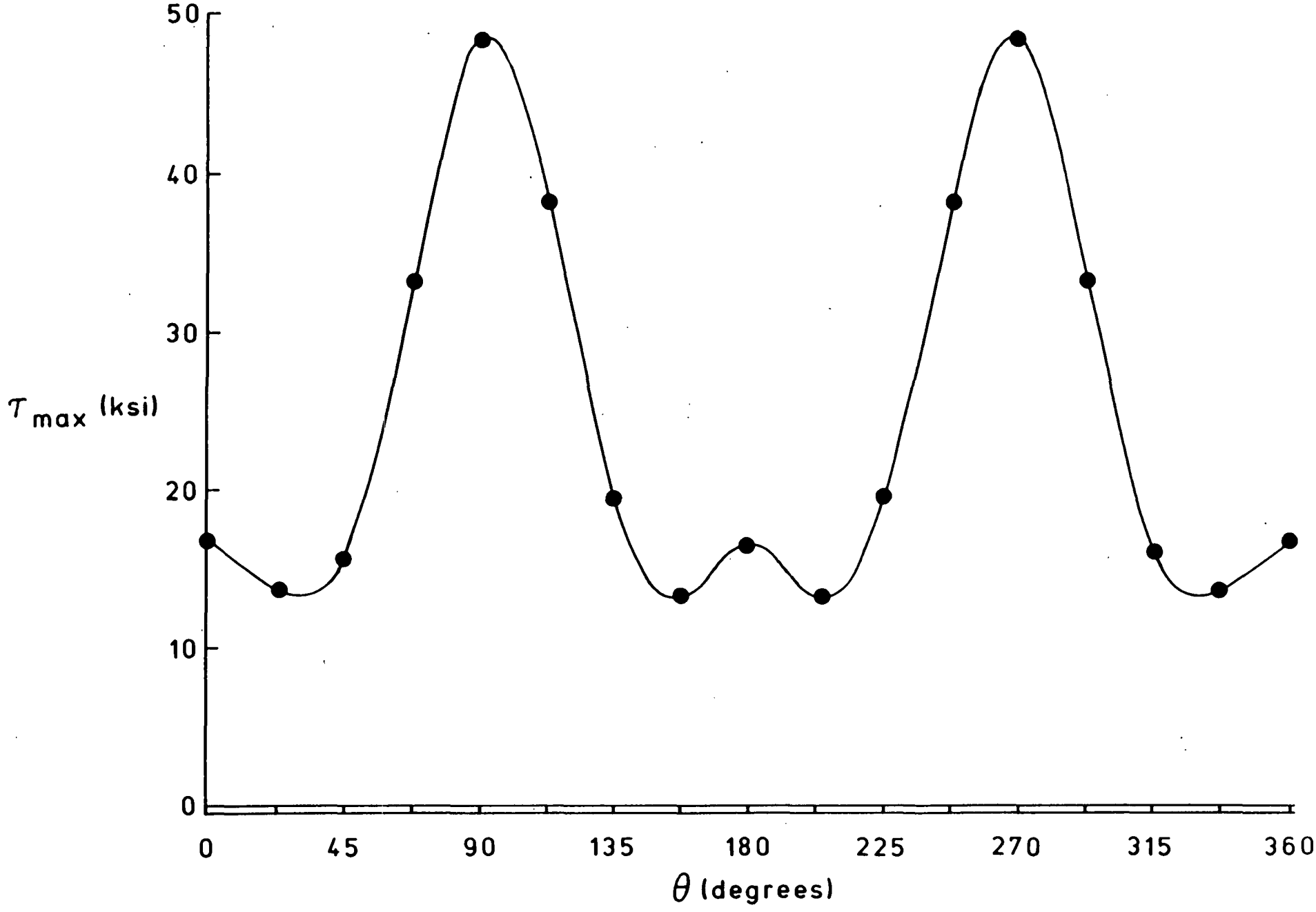

Figure 13. Maximum shear stresses around hole for 0^{o} ply-orientation for unstiffened composite panel

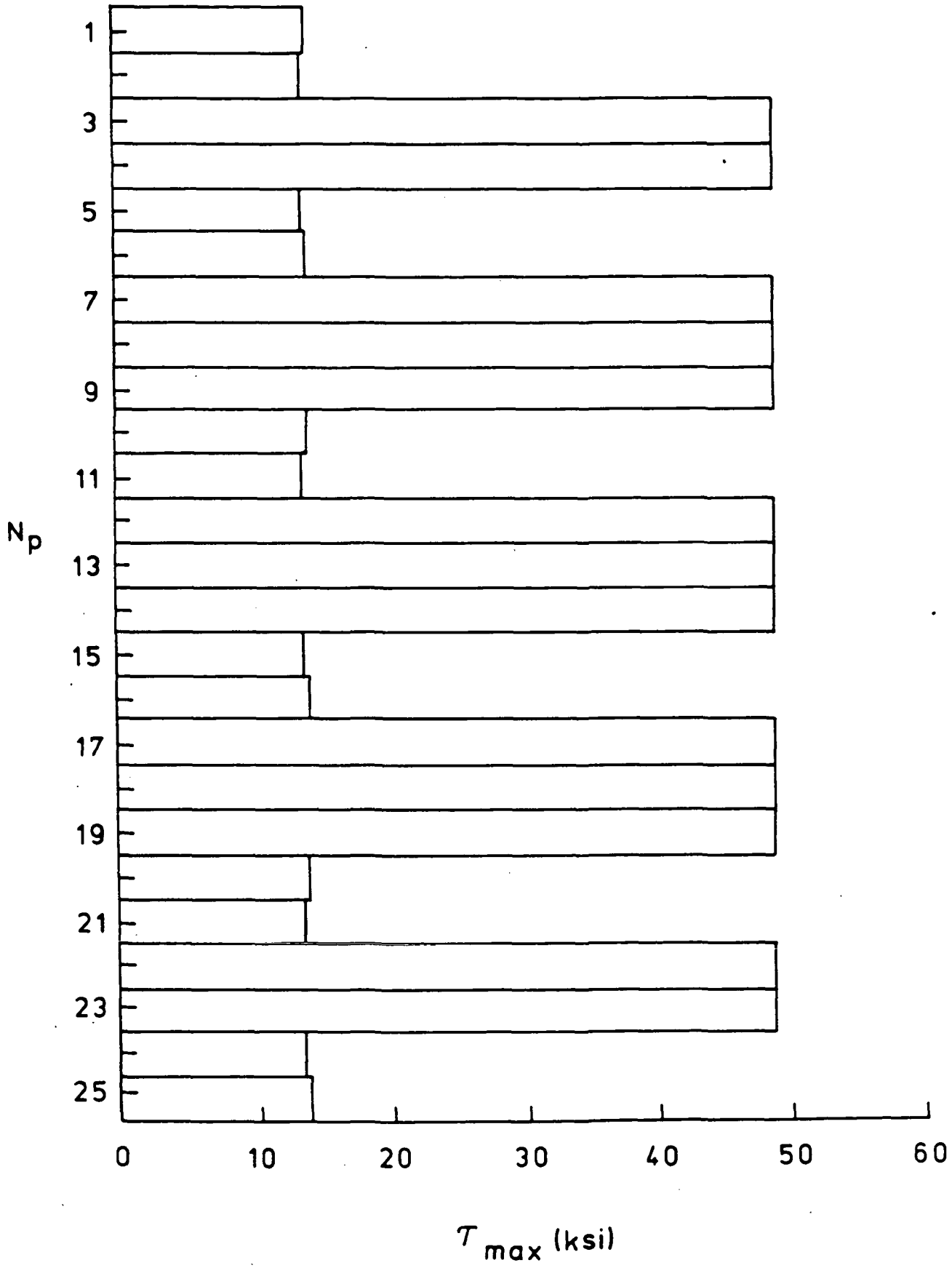

Figure 14. Maximum shear stresses for various layers of unstiffened composite panel

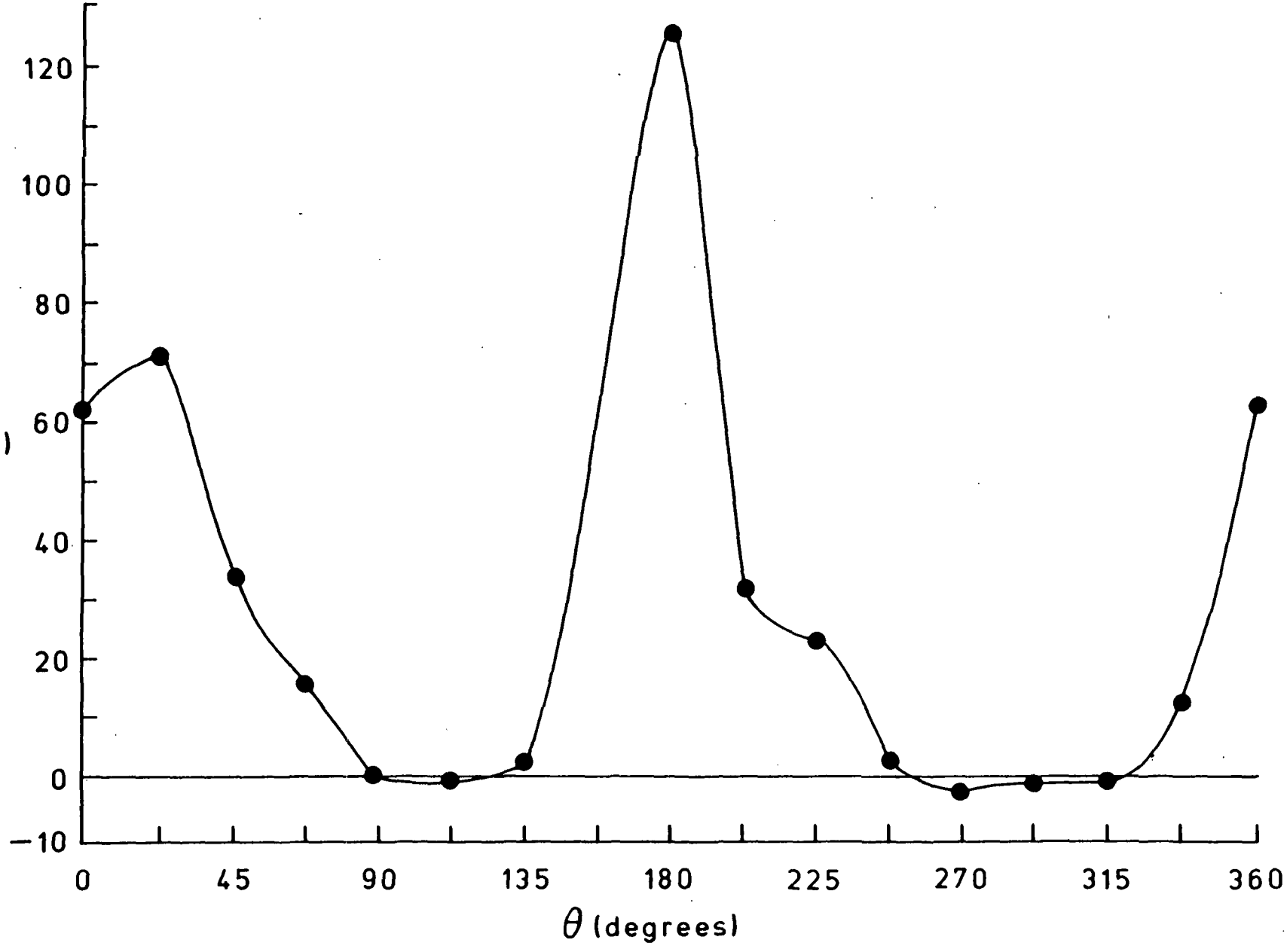

Figure 15. Maximum principal stresses around hole on 25th layer for stiffened composite panel

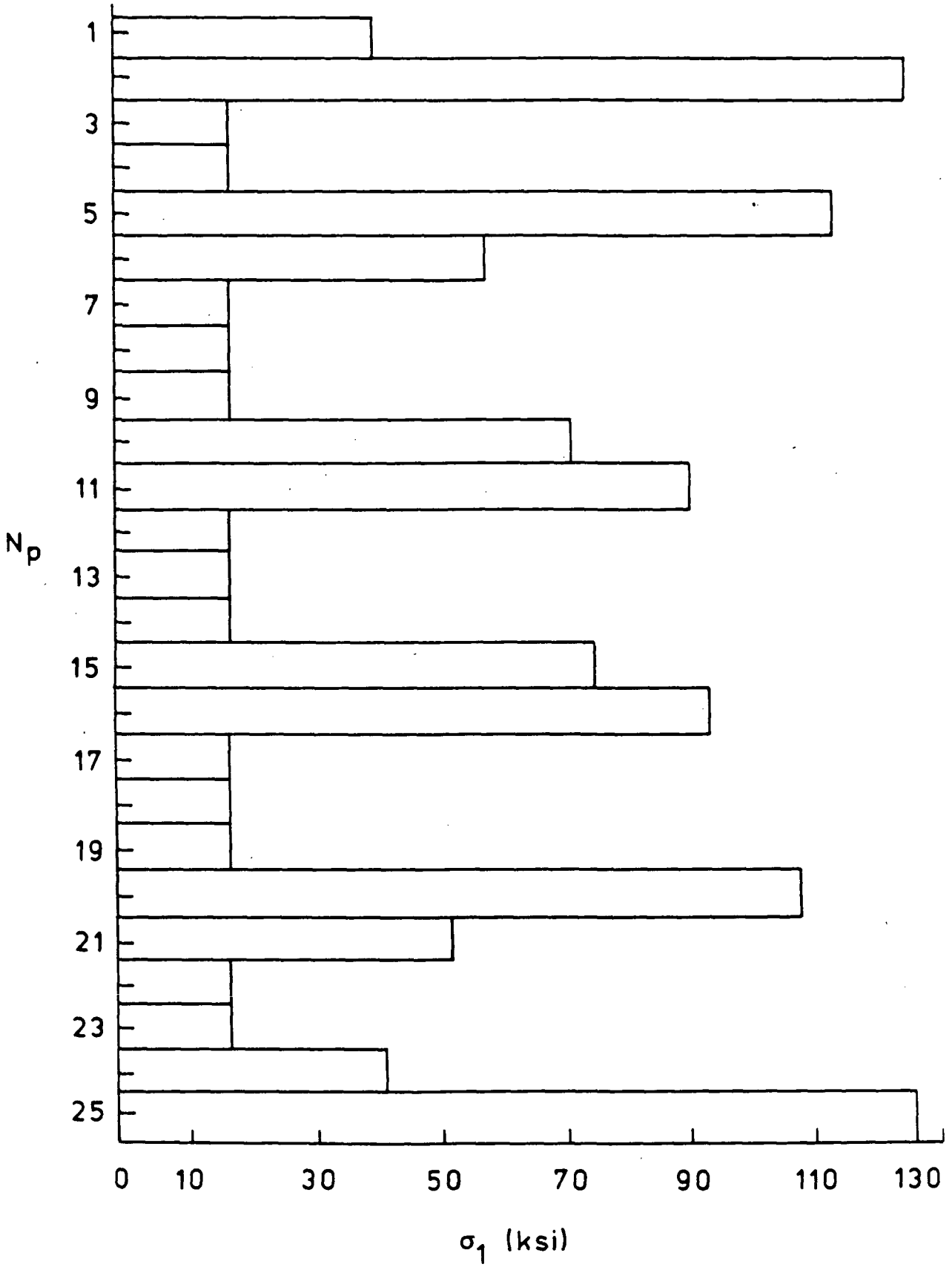

Figure 16. Maximum principal stresses for various layers of stiffened composite panel

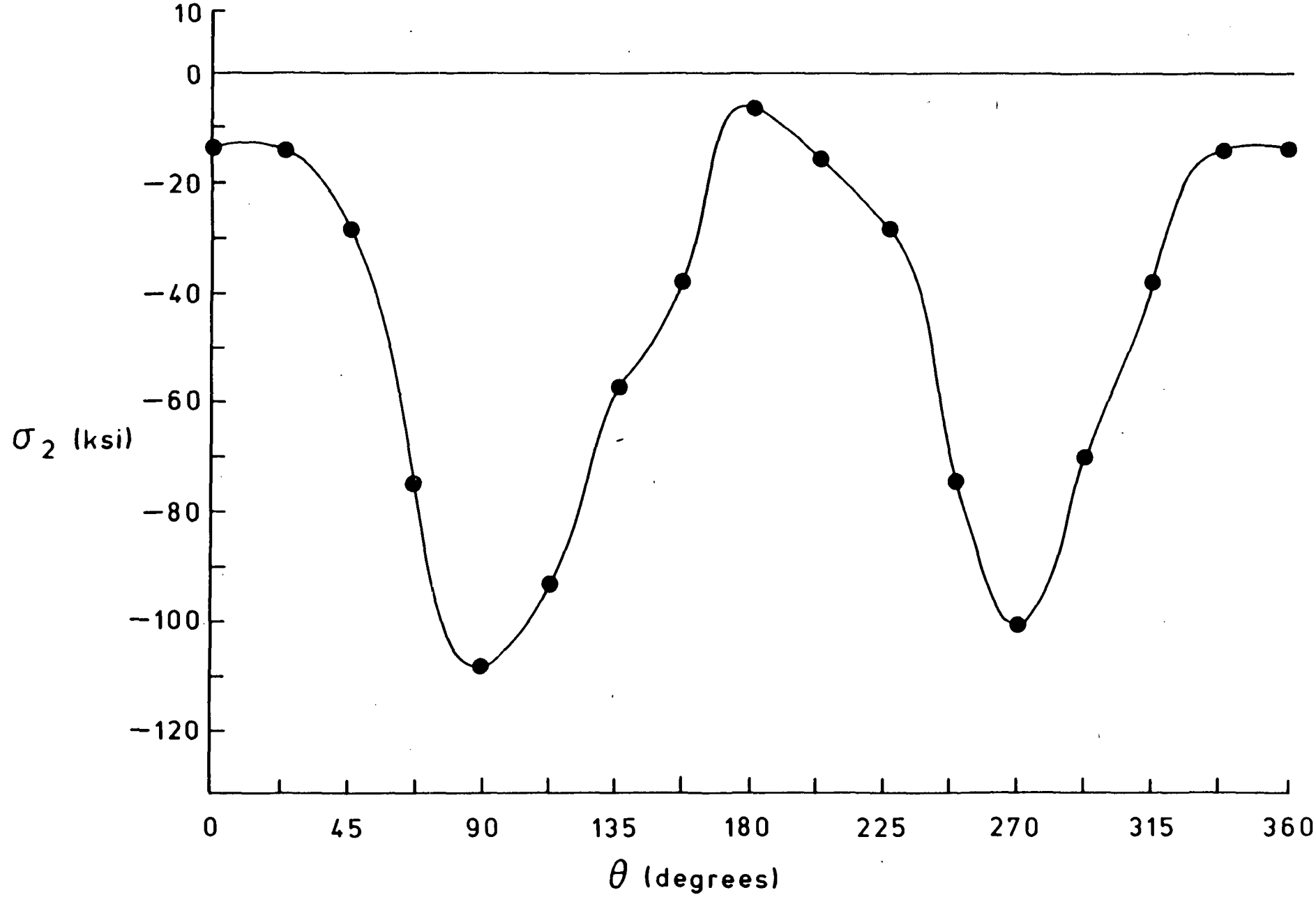

Figure 17. Minimum principal stresses around hole on 3rd layer for stiffened composite panel

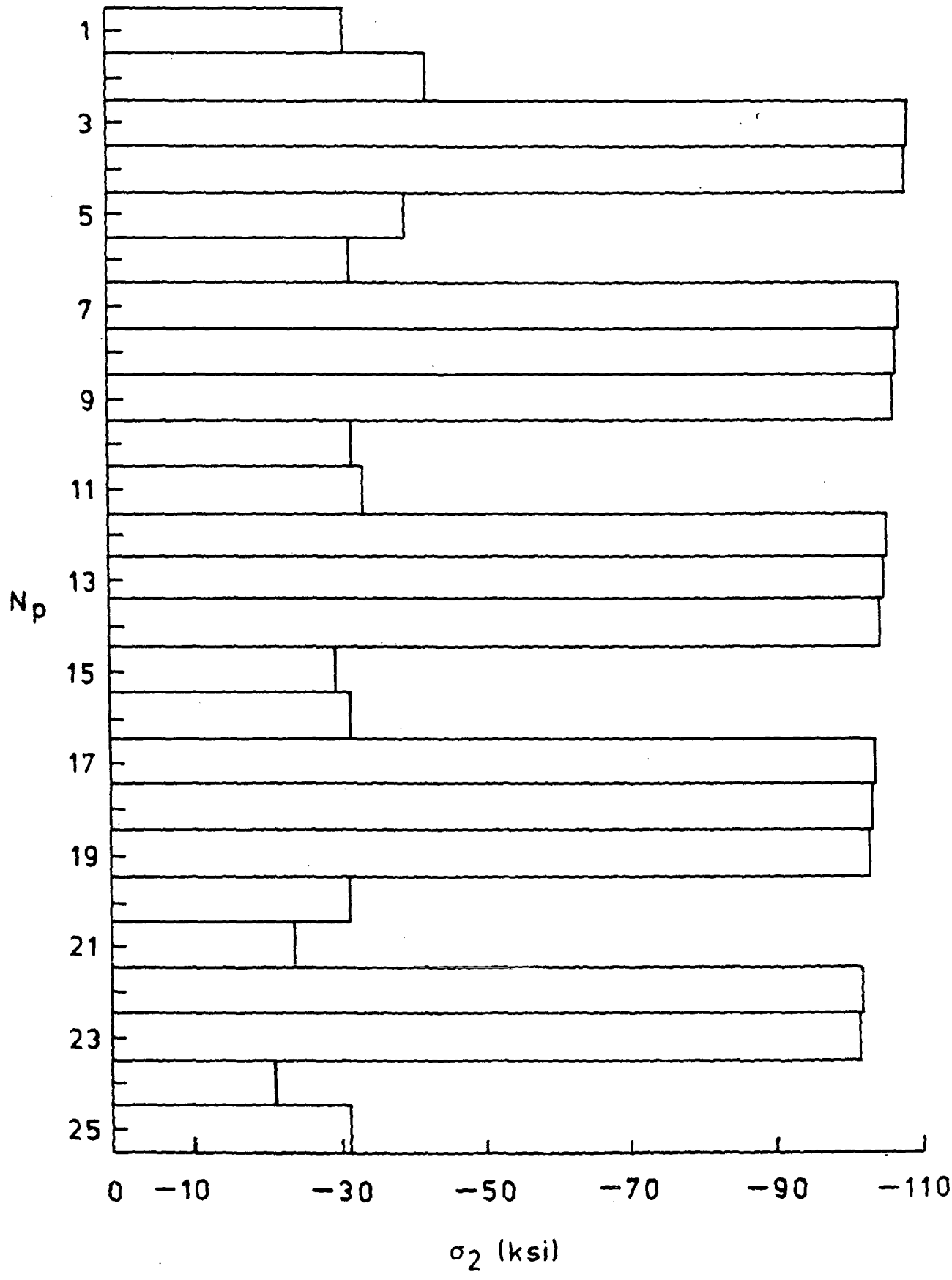

Figure 18. Minimum principal stresses for various layers of stiffened composite panel

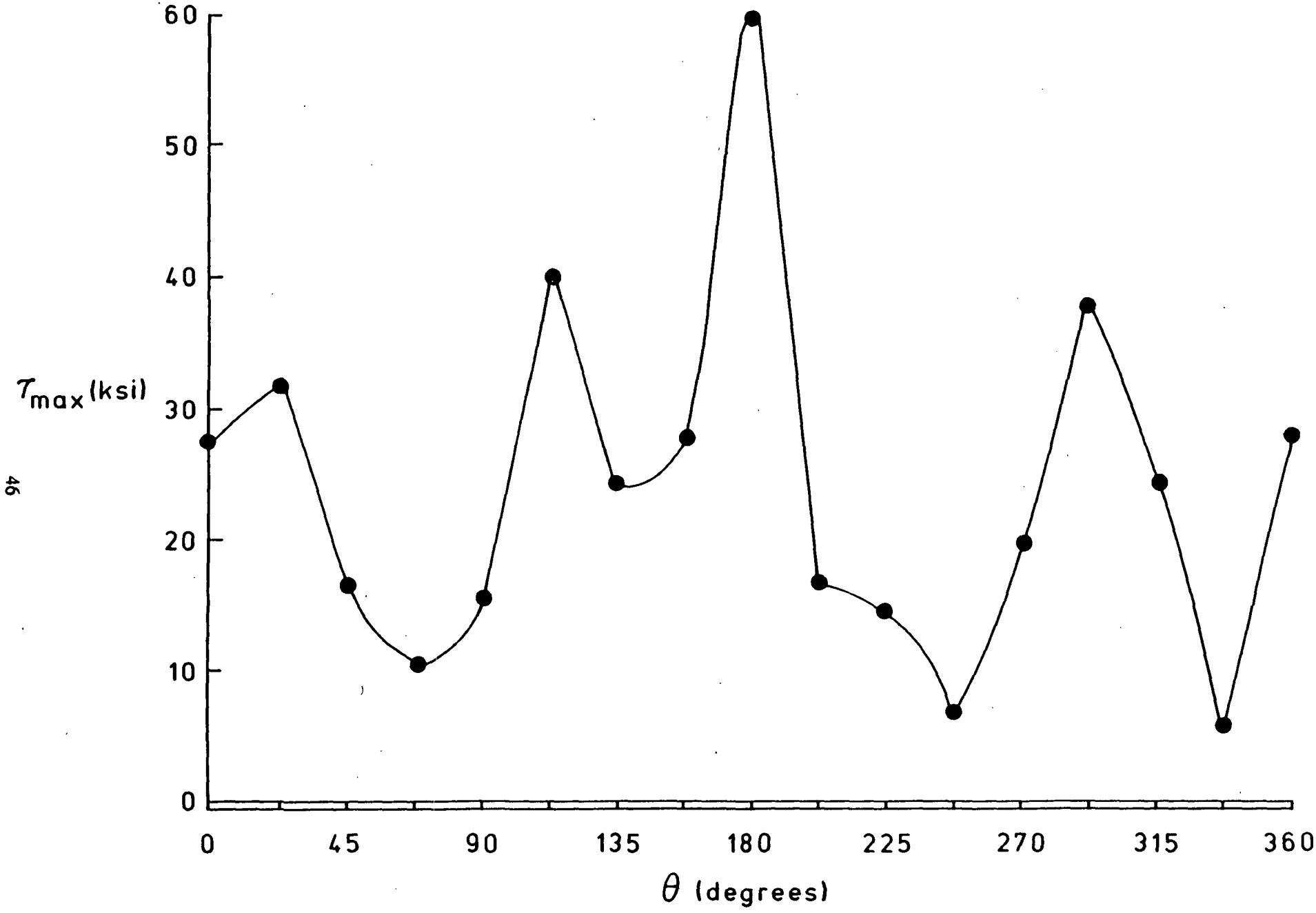

Figure 19. Maximum shear stresses around hole on 25th layer for stiffened composite panel

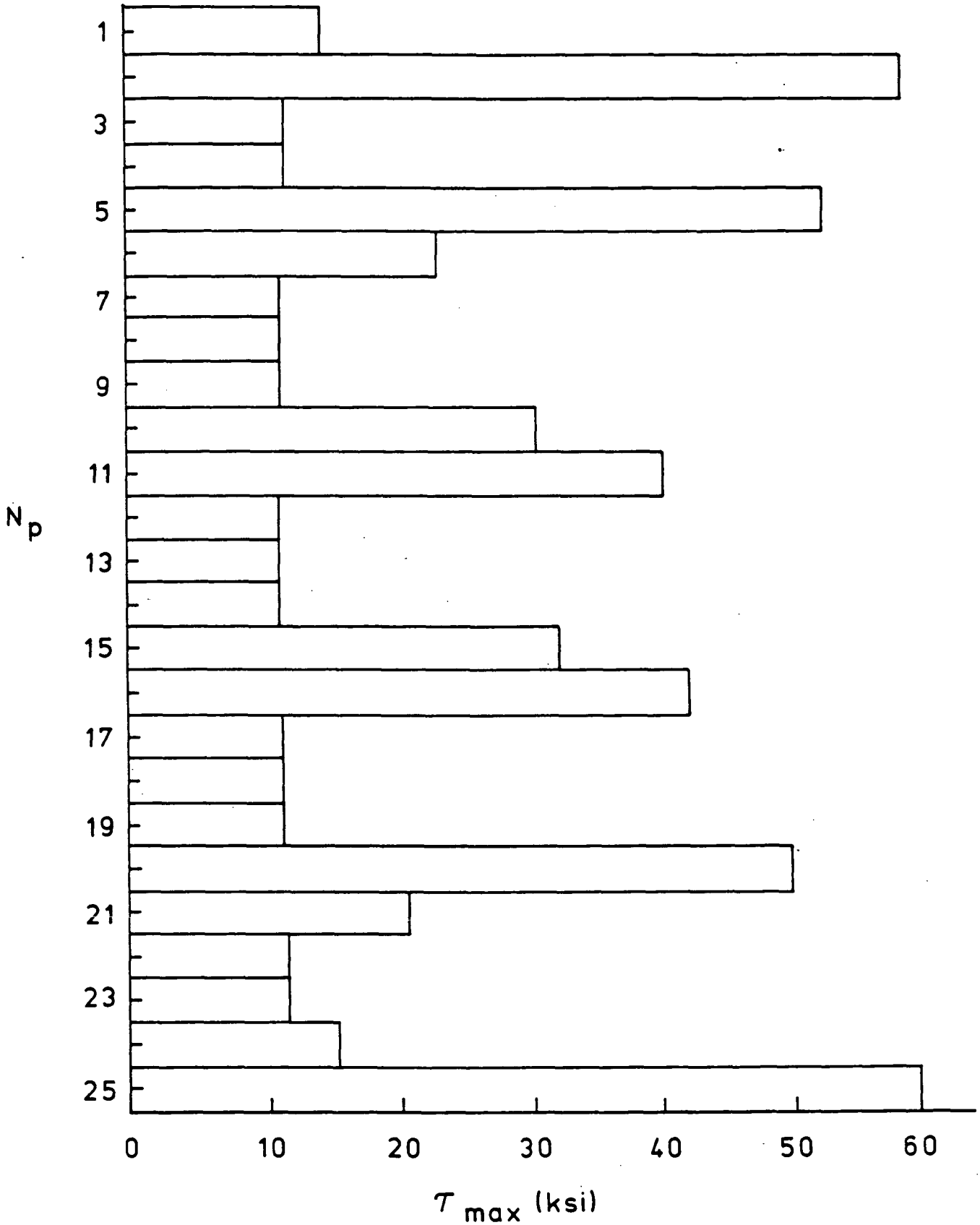

Figure 20. Maximum shear stresses for various layers of stiffened composite panel

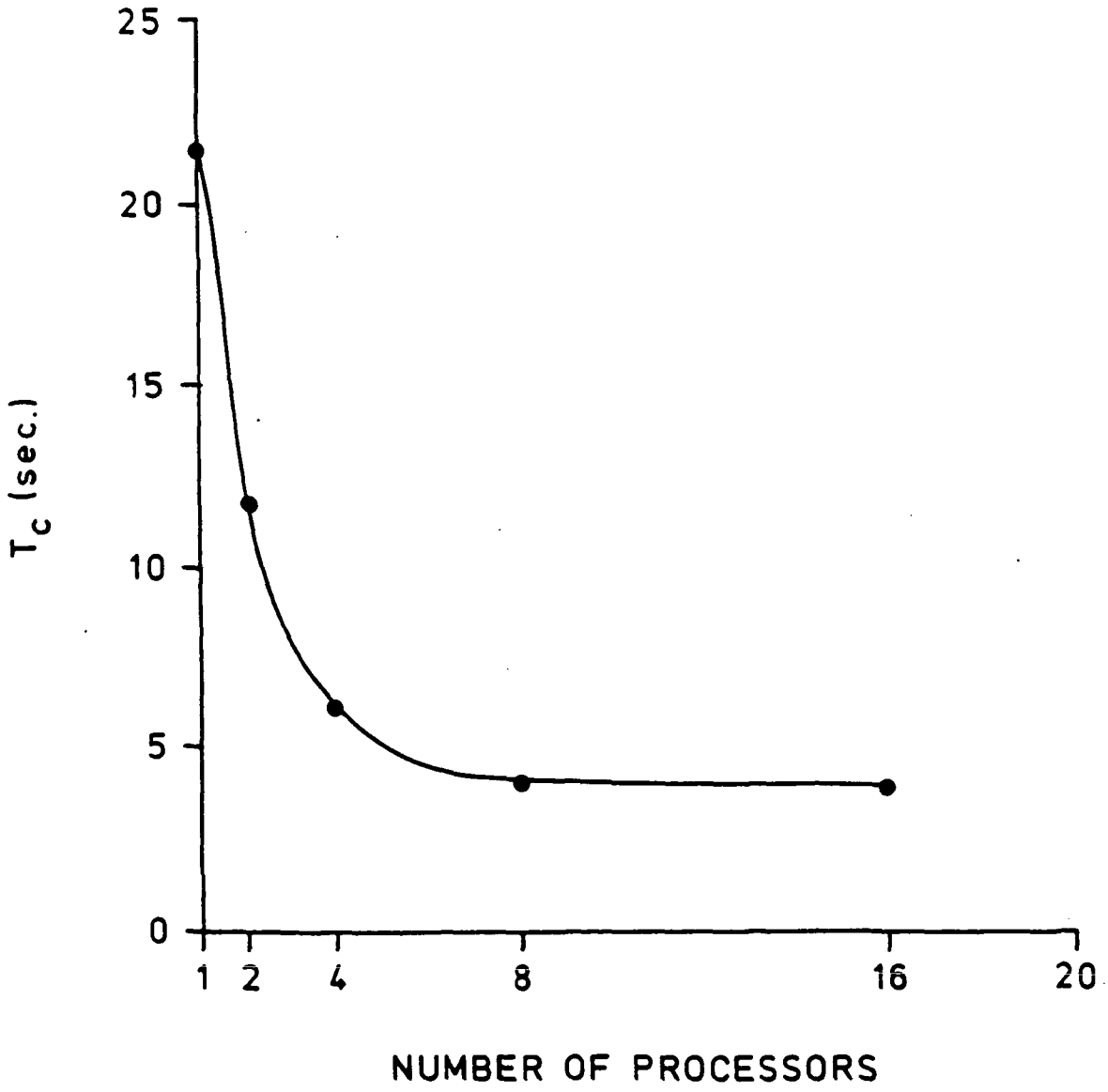

Figure 21. Computational time curve for unstiffened aluminum panel with hole

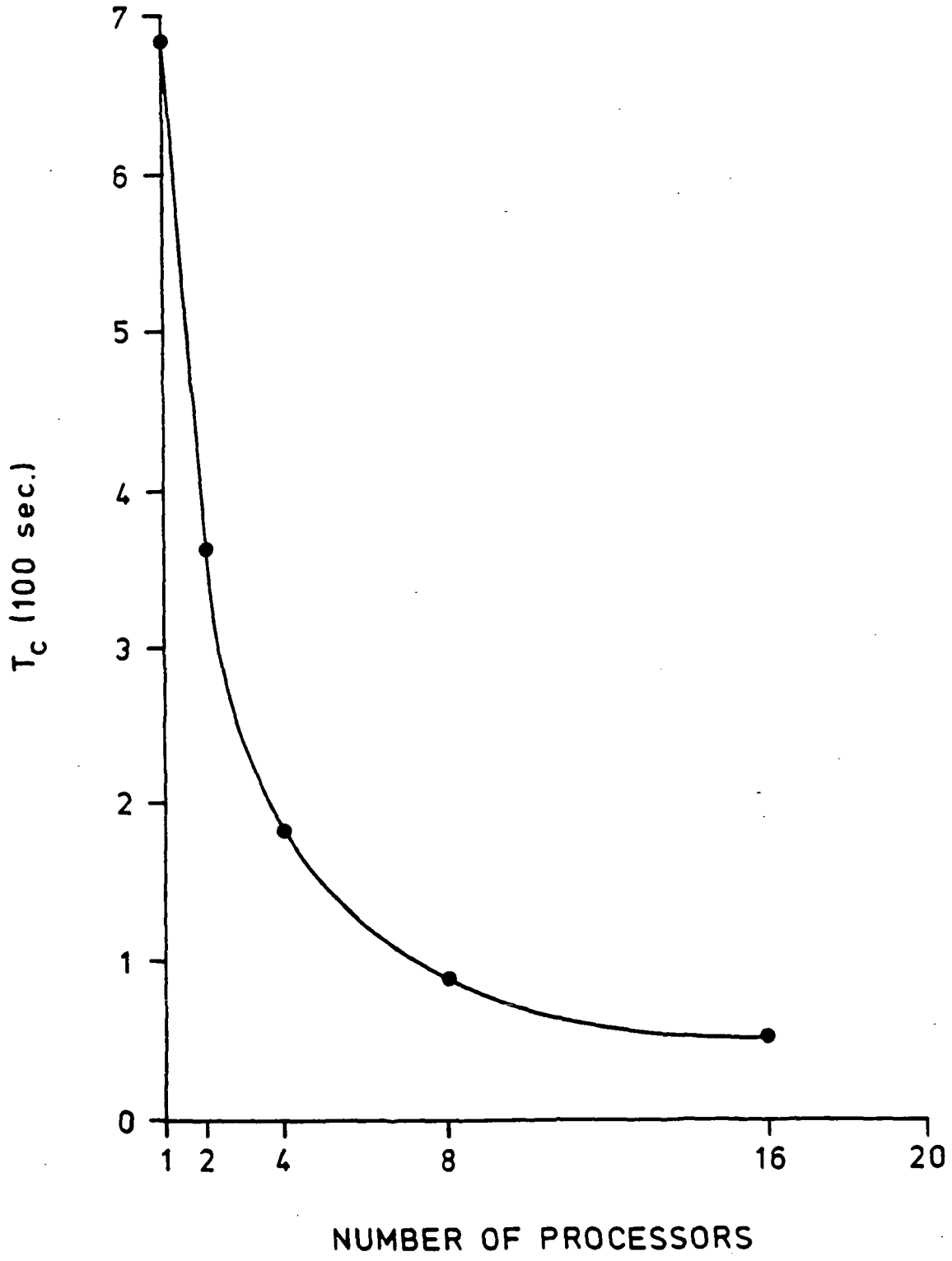

Figure 22. Computational time curve for stiffened aluminum panel with hole

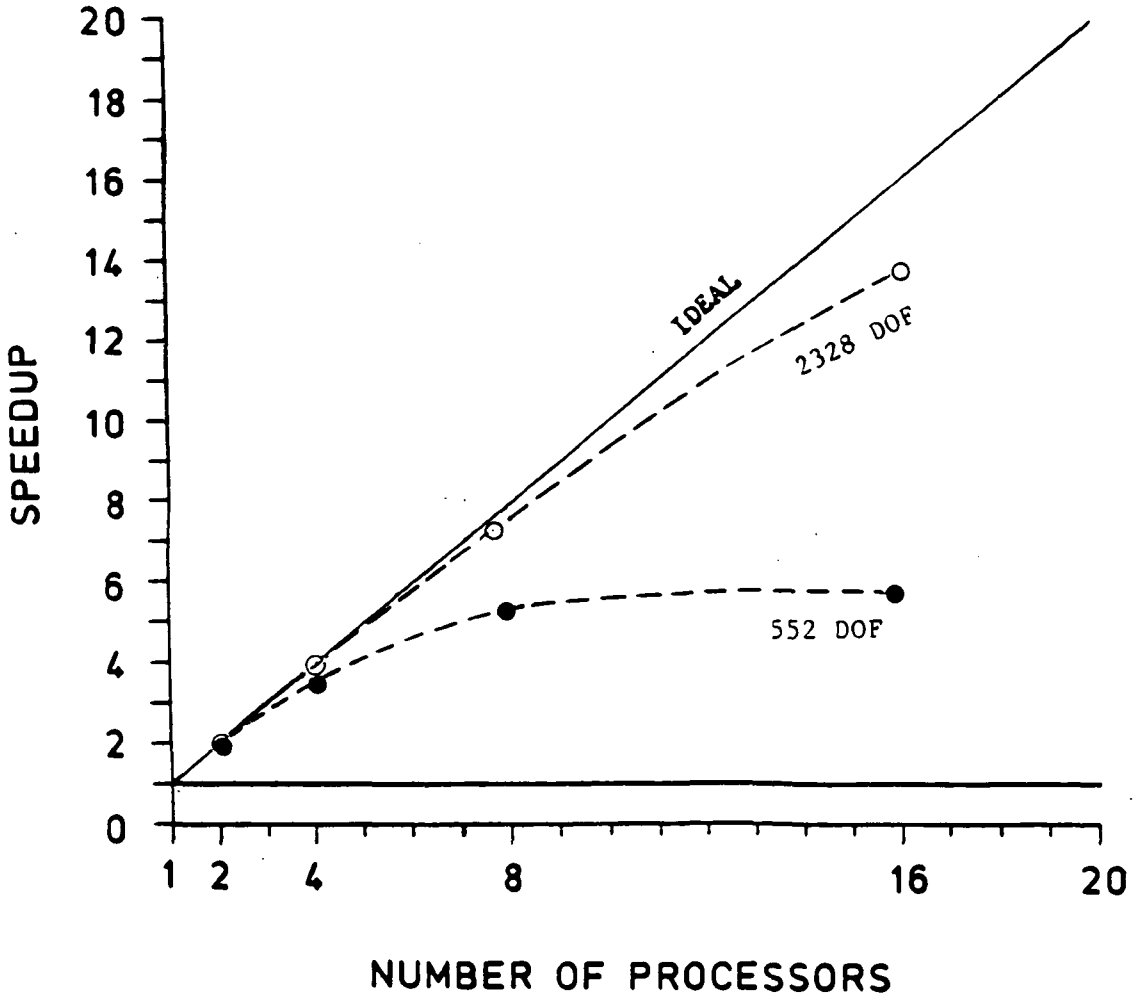

Figure 23. Speedup curves for unstiffened and stiffened aluminum panels with hole

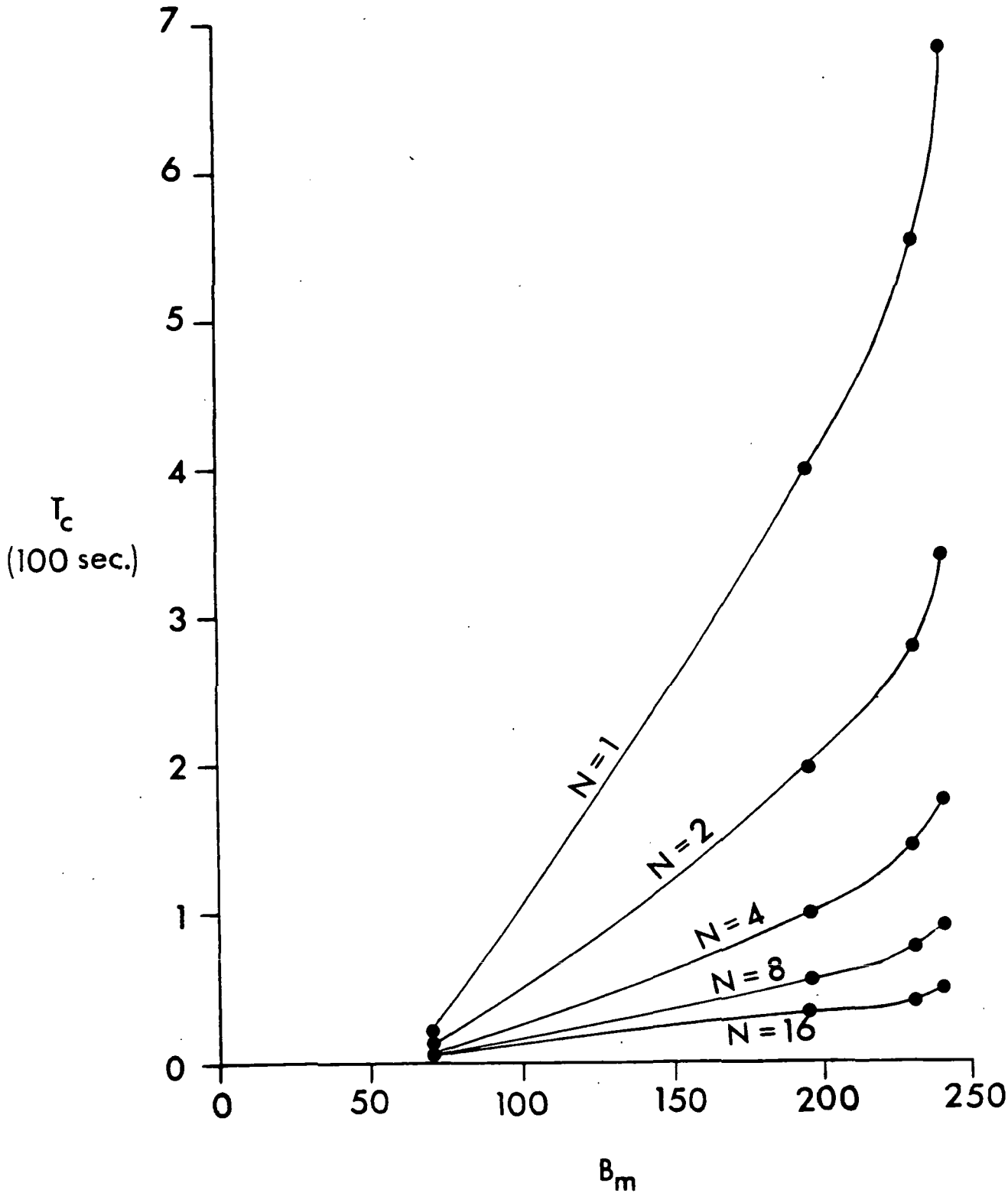

Figure 24. Variation of computational time with bandwidth and number of processors